Reactivity and loss mechanisms of NO_3 and N_2O_5 in a polluted marine environment: Results from in-situ measurements during NEAQS 2002

Mattias Aldener[1,2], Steven S. Brown[1] *, Harald Stark[1,2], Eric J. Williams[1,2], Brian M. Lerner[1,2], William C. Kuster[1], Paul D. Goldan[1], Patricia K. Quinn[3], Timothy S. Bates[3], Frederick C. Fehsenfeld[1], A. R. Ravishankara[1,2,4]

Abstract

Concentrations of NO_3 and N_2O_5 were measured using an *in-situ* instrument aboard the NOAA research vessel *Ronald H. Brown* in the marine boundary layer along the United States east coast as part of the New England Air Quality Study (NEAQS) in the summer of 2002. We analyze the results in terms of the loss partitioning and sink budgets for both of these compounds. Analysis of the data on nights with large N_2O_5 losses allowed for a determination of its heterogeneous uptake coefficient and gave $\gamma(N_2O_5) = 0.03 \pm 0.02$. Reactions of NO_3 with terrestrially-emitted biogenic VOC (isoprene, monoterpenes), advected into the marine boundary layer, and with DMS emitted from the ocean surface were also important. In general, loss of NO_3 and N_2O_5 was rapid, and the partitioning between NO_3 and N_2O_5 losses was roughly equal. Because rapid N_2O_5 loss consumes NO_x at twice the rate of the reaction of NO_2 with O_3, whereas rapid NO_3 loss leads to NO_x removal at the same rate, the equal partitioning of losses indicates a nocturnal NO_x loss rate of approximately 1.5 times the rate of NO_2 + O_3. Activation of halogens from the uptake of NO_3 and N_2O_5 on sea salt was calculated to have produced substantial amounts of active Cl on some mornings through the nocturnal formation and sunrise photolysis of $ClNO_2$ if the process proceeded at the rate determined by laboratory studies. However, there was no direct observational evidence to test the magnitude of the predicted source.

[1] NOAA Earth System Research Laboratory, Chemical Sciences Division, Boulder, Colorado, USA
[2] Cooperative Institute for Research in Environmental Sciences, University of Colorado, Boulder, Colorado, USA
[3] Pacific Marine Environmental Laboratory, Seattle, Washington, USA
[4] Department of Chemistry and Biochemistry, University of Colorado, Boulder, CO, USA
*Author to whom correspondence should be addressed. E-mail: steven.s.brown@noaa.gov

1. Introduction

The nitrate radical (NO_3) and dinitrogen pentoxide (N_2O_5) play a role in a number of important chemical processes within the troposphere, including the conversion of NO_x (=NO + NO_2) to nitric acid [*Platt and Heintz*, 1994; *Richards*, 1983; *Smith, et al.*, 1995], the nocturnal oxidation of VOC [*Winer, et al.*, 1984], the oxidation of dimethyl sulfide (DMS), emitted from the ocean surface, to sulfate aerosol [*Allan, et al.*, 1999; *Lucas and Prinn*, 2005; *Yvon, et al.*, 1996], and the growth of organic aerosol [*Moldanova and Ljungstrom*, 2000]. Formation and reactions of NO_3 and N_2O_5 primarily provide a nocturnal, non-photochemical pathway for these and other processes since photolysis and reaction with NO suppress formation of NO_3 in the presence of sunlight. Assessing and understanding the magnitude of these dark reactions in relation to their photochemical counterparts is an important, ongoing area of research.

The formation and subsequent reactions of NO_3 and N_2O_5 in the atmosphere have been detailed previously [*Wayne, et al.*, 1991]. Briefly, nitrogen dioxide oxidizes slowly ($k \sim 3\times10^{-17}$ cm^3 $molecule^{-1}$ s^{-1} at 298 K [*Sander, et al.*, 2003]) in the presence of ozone to form NO_3, which enters into a thermal equilibrium with NO_2 to reversibly form N_2O_5.

$$NO_2 + O_3 \rightarrow NO_3 + O_2 \qquad (1)$$

$$NO_3 + NO_2 \leftrightarrows N_2O_5 \qquad (2a, 2b)$$

Rapid reaction of NO_3 with NO (itself produced photolytically from NO_2) and efficient photolysis of NO_3 by visible light (lifetime in direct sunlight estimated at 5 s) effectively reverse the formation of NO_3 during sunlit hours.

$$NO_3 + NO \rightarrow 2NO_2 \qquad (3)$$

$$NO_3 + h\nu \rightarrow NO_2 + O \qquad (4a)$$

$$\rightarrow NO + O_2 \qquad (4b)$$

Nocturnal mixing ratios of NO_3 may range into the tens or even hundreds of pptv, while those of N_2O_5 may exceed 1 part per billion by volume (ppbv). At these levels, NO_3

becomes an important oxidant, particularly for unsaturated VOC (e.g., those of biogenic origin) and for dimethyl sulfide (DMS) over the oceans. The primary loss process for N_2O_5 is hydrolysis to form nitric acid; this reaction is a significant pathway for the conversion of NO_x (= NO and NO_2) to HNO_3, both regionally and globally [*Dentener and Crutzen*, 1993]. Figure 1 summarizes these reactions.

Our recently developed, *in-situ* instrument for the detection of both NO_3 and N_2O_5 [*Brown, et al.*, 2002] was deployed for its first major field campaign during the New England Air Quality Study in 2002 (NEAQS 2002). The measurement platform was the NOAA research vessel *Ronald H. Brown* (R/V *Brown*), which sailed off the U. S. East Coast, with a particular emphasis on the New England area, during a 4 week intensive measurement period in July and August, 2002. In two previous manuscripts, we quantified the nocturnal oxidation of NO_x to HNO_3 in the marine environment [*Brown, et al.*, 2004], and the daytime and nighttime oxidation of VOC [*Warneke, et al.*, 2004]. A forthcoming manuscript will discuss the influence of NO_3 oxidation of DMS to the sulfur budget in a polluted marine environment [*Stark, et al.*, 2006]. The goal of this manuscript is to explore the reactions of NO_3 and N_2O_5 in more detail, with particular attention to the different loss mechanisms for these compounds and the influence of these reactions on nocturnal NO_x and VOC processing within polluted air masses.

2. Measurements of NO_3 & N_2O_5

Concentrations of NO_3 and N_2O_5 were measured by cavity ring-down spectroscopy (CaRDS) using a previously described instrument [*Brown, et al.*, 2002]. CaRDS is a high sensitivity direct absorption technique based on the measurement of the time constant, τ, for single-exponential decay of light intensity from a high finesse optical cavity [*Busch and Busch*, 1999]. Our instrument uses a pulsed laser system (Nd:YAG laser pumped dye laser) resonant with the peak of NO_3 absorption spectrum near 662 nm to pump two separate optical cavities. One of these cavities is used to measure NO_3 via its 662-nm absorption from an inlet at ambient temperature, and the other is used to measure the sum of NO_3 + N_2O_5 from an inlet heated to 75 °C to induce thermal decomposition of N_2O_5 to NO_3. For the NEAQS 2002 sampling conditions, the

instrument sensitivity was 0.5 - 2 pptv for NO_3 (5 s average) and 2-5 pptv for N_2O_5. The sensitivity range was limited by turbulent flow noise encountered under the conditions of this campaign and was somewhat larger than we have reported previously for this instrument.

An important limitation to the accuracy of the NO_3 and N_2O_5 measurements during NEAQS 2002 was the inlet transmission efficiency, T_E. The CaRDS instrument, like many of the other gas-phase measurements, was housed in a sea container on an upper deck in the forward part of the ship. An air sample was drawn from a point above and immediately in front of the sea container (11 m above the sea surface) through a fast flow (300 standard liters per minute, SLPM) system consisting of 3 m of 3/4" OD PFA Teflon tubing. This inlet was exchanged regularly (every 2-3 days), and losses of NO_3 and N_2O_5, measured from the dependence of the signal on the flow rate through the system and on the length of the inlet tubing, were < 10% (T_E estimated at 0.95 ± 0.05). Sample flows were drawn from the fast-flow manifold through 1" OD halocarbon wax-coated Pyrex tubing at 12 SLPM and 5-8 SLPM for the measurement of NO_3 (ambient temperature) and the sum, $NO_3 + N_2O_5$ (heated to 75 °C), respectively. Unanticipated turbulent flow noise in the heated channel required reduction of this flow rate from its optimum of 12 SLPM. Laboratory characterization of the losses in this system prior to the campaign showed transmission efficiencies of 90 ± 5%; however, transmission tests carried out during and after the campaign showed that aging of the halocarbon wax surfaces led to a degradation of the T_E to 80 ± 15% for NO_3 and 60 ± 20% for $NO_3 + N_2O_5$. Each sample flow also passed through a Teflon membrane filter to suppress optical extinction at 662 nm from atmospheric aerosol. Filters were changed at regular, 1-hour intervals using a manual device. Field tests conducted during NEAQS 2002 confirmed previously measured filter transmission efficiencies of 85 ± 10% for NO_3 and > 99% for N_2O_5. The net transmission efficiency through the entire sampling system for NO_3 and N_2O_5 were 60% and 55%, respectively, and the corresponding uncertainties in the reported concentrations (based on propagation of the errors listed above) are 35% for NO_3 and 40% for N_2O_5. In the time since the 2002 campaign, the inlet system has been redesigned to increase the NO_3 and N_2O_5 inlet transmission efficiency (70% and 85%,

respectively) and the measurement accuracy (25% and 20%, respectively) [*Dubé, et al.*, 2006].

3. Data Overview

The R/V *Brown* sailed from Charleston, S.C. on July 12, 2002, made a port call in Portsmouth, N.H. from July 26-29, and returned to Charleston on August 11. Excluding the period during the port call, the R/V *Brown* sampled in the area of the Massachusetts, New Hampshire and Maine coastlines from July 17 to August 7, the area near New York City from July 14–17 and Norfolk, VA from August 9-10, 2002. Figure 2 shows the ship track within the intensive study area. The suite of instruments on board the R/V *Brown* that were relevant to the analysis in this manuscript included *in-situ* measurements of O_3, NO, NO_2 and NO_y (i.e., the sum of reactive nitrogen) by chemiluminescence at 1-min time resolution [*Thornton, et al.*, 2003], HNO_3 by mist chamber at 5-min resolution [*Dibb, et al.*, 2004], speciated VOC by GC-MS (5 min resolution each 30 minutes) [*Goldan, et al.*, 2004], aerosol size distributions from a series of mobility analyzers and particle counters at 15 min time resolution, and aerosol composition from a Particle into Liquid Sampler (PiLS) and an Aerosol Mass Spectrometer (AMS) [*Bates, et al.*, 2005].

Figure 3 shows an overview of the measured mixing ratios of NO_3 and N_2O_5 during the entire campaign. There are no data reported for the period from July 19-26 because of technical difficulties with the instrument. The mixing ratios of NO_3 and N_2O_5 ranged from the instrument detection limit up to 140 pptv and 1.6 ppbv, respectively. Concentrations of both species exhibited considerable variability, due to the variety of different source regions sampled (e.g., urban outflow vs. clean marine) and due to the variability of the chemical composition (i.e., NO_x, O_3, VOC, etc.) within each of the different air masses. The dominant flow in the New England region was offshore, impacted by emissions from the urban corridor between Washington, D. C. and Boston, MA, but air masses from Canada and from the Atlantic Ocean (as identified by back trajectory analysis) were also encountered.

4. Lifetimes and First-Order Loss Rate Coefficients for NO_3 and N_2O_5

One of the most common and useful diagnostics in the analysis of atmospheric NO_3 and N_2O_5 is their steady-state lifetime [*Platt, et al.*, 1984], or the ratio of their concentrations to their source strength (molecules cm^{-3} s^{-1}) from the reaction of NO_2 with O_3 (reaction 1). Because NO_3 and N_2O_5 are a closely coupled pair that interconvert rapidly, the lifetime of each depends on the loss rate for the other. At steady-state, the loss frequency is equal to the concentration over the production rate. Taking a single, first order loss rate coefficient, k_{NO_3}, to describe the sum of all of the losses for NO_3, and a separate first-order loss rate coefficient, $k_{N_2O_5}$, to parameterize the losses for N_2O_5, the following two equations give an approximate relationship between the observed steady-state lifetimes and the sinks for NO_3 and N_2O_5 [*Brown, et al.*, 2003; *Heintz, et al.*, 1996].

$$\tau_{NO_3} \equiv \frac{[NO_3]}{k_1[NO_2][O_3]} \approx (k_{NO_3} + k_{N_2O_5}K_{eq}[NO_2])^{-1} \quad (5)$$

$$\tau_{N_2O_5} \equiv \frac{[N_2O_5]}{k_1[NO_2][O_3]} \approx \left(k_{N_2O_5} + \frac{k_{NO_3}}{K_{eq}[NO_2]}\right)^{-1} \quad (6)$$

Here K_{eq} is the temperature dependent equilibrium constant for the equilibrium between NO_2, NO_3 and N_2O_5 (reaction 2). A derivation of these equations can be found in [*Brown, et al.*, 2003].

Equations (5-6) show that, presuming NO_3 and N_2O_5 have achieved steady state, the individual loss rate coefficients, k_{NO_3} and $k_{N_2O_5}$, may be determined as the intercept and slope of a linear fits to a plot of $\tau_{NO_3}^{-1}$ against $K_{eq}[NO_2]$, or as the slope and intercept of a plot of $\tau_{N_2O_5}^{-1}$ against $(K_{eq}\times[NO_2])^{-1}$ [*Brown, et al.*, 2006]. The steady state approximation was likely valid for most of the NEAQS 2002 data (average nocturnal temperature = 295 K, nocturnal NO_2 from 0.2 – 30 ppbv, average ~ 4 ppbv). A box model analysis showed that the time required to approach steady state for most conditions encountered during NEAQS 2002 was ≤ 1 hour, except for very weak sinks for NO_3 and N_2O_5, as described in section 5.3 below. Determination of average loss rate

coefficients from the observed NO_2 dependence of the steady state lifetimes according to equations (5-6) was complicated by variability in the sinks for NO_3 and N_2O_5 relative to the independent variable, $K_{eq}[NO_2]$, in equations (5-6). This effect was apparent from scatter in the observed steady state lifetimes that tended to obscure their NO_x scaling. Only a limited number of cases showed a clear dependence on NO_x outside of this scatter. For most cases, we have simply calculated the total losses for NO_3 and N_2O_5 from the right hand side of equations (5-6) as described below and compared them to observed steady-state lifetimes on the left hand side of these equations.

The first order loss rate coefficients can be calculated from measurements of the known sinks for NO_3 and N_2O_5 (i.e., VOC and aerosol). These calculated values will be referred to as $k_{NO_3}^{Calc}$ and $k_{N_2O_5}^{Calc}$. In the case of NO_3, the calculated loss rate coefficient is the sum of the measured hydrocarbons (including DMS) and NO concentrations multiplied by their temperature-dependent rate coefficients for reaction with NO_3 ($k_i(T)$ and $k_{NO}(T)$, respectively) [*Atkinson*, 1991]. With the exception of ship plumes containing recently-emitted NO_x, NO was below its detection limit during nighttime hours, and reaction of NO_3 with NO (reaction 3) has been neglected for the analysis of nighttime NO_3 measurements. Photolysis (reaction 4) was also negligible at night. First-order heterogeneous loss for NO_3 on aerosol surface has been included using an assumed uptake coefficient for NO_3, $\gamma(NO_3) = 4\times10^{-3}$ [*Allan, et al.*, 1999; *Rudich, et al.*, 1996]. The aerosol surface area density, A ($\mu m^2\ cm^{-3}$), was calculated from the measured, RH corrected, number and size distributions (up to 10 μm), assuming spherical particles.

$$k_{NO_3}^{Calc} = \sum_i k_i(T)[VOC_i] + \frac{1}{4}\bar{c}A\gamma(NO_3) \qquad (7)$$

The first term is predicted to be by far the most important contribution at night, and is analyzed in detail in the following sections. Heterogeneous uptake of NO_3, calculated from the literature uptake coefficient given above, is small by comparison; however, relatively little is known about this uptake coefficient on real atmospheric aerosol; if it were large (i.e., 0.04 rather than 0.004), heterogeneous uptake of NO_3 would be competitive with gas-phase reactions of NO_3 with VOC. The form of the NO_3

heterogeneous loss term is the same as that described below for N_2O_5 hydrolysis, except that it has not been corrected for gas-phase diffusion because the smaller uptake coefficient renders this correction negligible.

The $k_{N_2O_5}^{Calc}$ include only the loss due to heterogeneous hydrolysis of N_2O_5 on aerosol, corrected for gas-phase diffusion to the particles [*Fuchs and Stugnin*, 1970].

$$k_{N_2O_5}^{Calc} = \bar{c}\gamma(N_2O_5)\sum_i N_i \pi r_i^2 \left\{1 + \gamma(N_2O_5)\frac{0.750 + 0.283K_n(r_i)}{K_n(r_i)[K_n(r_i)+1]}\right\}^{-1} \quad (8)$$

$$K_n(r_i) = \frac{3D}{r_i\bar{c}} \quad (9)$$

Here N_i is the number density of particles (particles cm^{-3}) in the size bin with average radius r_i, K_n is the Knudsen number, $\bar{c}$ is the mean molecular speed and D is the gas phase diffusion coefficient for N_2O_5. Equation (8) reduces to a simpler form in the limit where gas phase diffusion to the particle can be neglected, for small particles and small uptake coefficients.

$$k_{N_2O_5}^{calc} = \frac{1}{4}\bar{c}A\gamma(N_2O_5) \quad (10)$$

Although the differences between equations (8) and (10) were always less than 5%, N_2O_5 uptake was calculated using equation (8). Dry deposition (i.e., for uptake by the ocean surface) for either NO_3 or N_2O_5 has not been included in the calculated loss rate coefficients. Assuming a 100 m depth for the marine boundary layer in the Gulf of Maine [*Angevine, et al.*, 2004], and a deposition velocity for NO_3 and/or N_2O_5 of ~ 1 cm s^{-1}, similar to that for nitric acid in this region [*Brown, et al.*, 2004], the predicted lifetime with respect to deposition is 2.5 hours [*Wesely and Hicks*, 2000]. This loss is 10-1000 times smaller than calculated losses due to VOC and aerosol. However, stratification and reduced mixing of marine air masses within the shallow boundary layer could lead to vertical gradients in NO_3, N_2O_5 and/or their sources and sinks that in turn could complicate the analysis of NO_3 and N_2O_5 sink budgets because of uncertainties in the

rates of mixing processes between adjacent, inhomogeneous air masses [*Geyer and Stutz*, 2004]. These possible effects have not been included in this analysis.

Observed lifetimes, τ_{NO_3} and $\tau_{N_2O_5}$, are defined as in equations (5-6) as the ratios of the observed concentrations to the source strengths. The calculated lifetimes, $\tau_{NO_3}^{Calc}$ and $\tau_{N_2O_5}^{Calc}$, are from the right hand side of these equations, using the calculated first order loss rate coefficients, $k_{NO_3}^{Calc}$ and $k_{N_2O_5}^{Calc}$, temperature-dependent equilibrium constant, $K_{eq}(T)$, and the measured NO_2 concentrations. Figure 4 shows a comparison of the observed to the calculated lifetimes for the entire NO_3 and N_2O_5 data set. The calculated lifetimes have $\gamma(N_2O_5)$ held fixed at a value of 0.03 throughout (see section 5.1). Observed lifetimes were generally in a range of a few minutes, similar to previous measurements of NO_3 lifetimes by DOAS at surface sites [*Allan, et al.*, 1999; *Geyer, et al.*, 2001; *Heintz, et al.*, 1996; *Martinez, et al.*, 2000]. The observed lifetimes also generally agree with the calculations, although there are cases in which the observed lifetimes are either shorter than or longer than the calculations, as discussed below.

The next section deals with the description and accounting of the known sinks and inferences about potential unknown sinks on a more detailed, night by night basis. Characterization of the relationship between the overall lifetimes of NO_3 and N_2O_5 and the specific sinks of either compound is important for several reasons. First, NO_3 is a strong nocturnal oxidant; comparison of observed and calculated losses of NO_3 due to reaction with VOC helps to assess the degree to which this nocturnal oxidation is understood. Second, the determination of N_2O_5 loss rates, in combination with the aerosol surface area, gives a measurement of the N_2O_5 uptake coefficient based solely on atmospheric observations. This reaction is important for the conversion of NO_x to HNO_3. Finally, the balance between NO_3 and N_2O_5 losses determines the efficiency of nocturnal NO_x removal. Under conditions where NO_3 and N_2O_5 react rapidly, this loss is rate limited by the reaction of NO_2 with O_3 [*Brown, et al.*, 2004].

$$\frac{d[NO_x]}{dt} = -Sk_1[O_3][NO_2] \tag{11}$$

$$S = 1 + \frac{k_{N_2O_5}K_{eq}[NO_2]}{k_{NO_3} + k_{N_2O_5}K_{eq}[NO_2]} \tag{12}$$

Assuming that NO_3-VOC reactions irreversibly remove NO_x (i.e., that they do not regenerate NO_2), the factor S varies between 1 in the limit where NO_3 losses are rapid relative to those for N_2O_5 and 2 for the opposite case (i.e., hydrolysis of N_2O_5 removes 2 NO_x, whereas irreversible reaction of NO_3 consumes only one). Therefore, the relative importance NO_3 and N_2O_5 sinks makes a difference of up to a factor of two to nocturnal lifetime of NO_x.

5. Case-by-case Studies

5.1 Case 1: Losses dominated by N_2O_5 hydrolysis

There were several nights on the 2002 campaign characterized by relatively slow loss of NO_3 in comparison to hydrolysis of N_2O_5. A sink budget analysis on these nights yields a determination of the heterogeneous uptake coefficients for N_2O_5 , $\gamma(N_2O_5)$. Figure 5 shows an example from the time series of NO_3, N_2O_5, NO_2 and O_3 mixing ratios (averaged to 1 min resolution) on July 29-30, 2002. The bottom left graph shows a map of the ship track during this period, color coded according to N_2O_5. The air flow was mainly out of the W and NW, as calculated by the backward trajectories shown on the map [*Draxler and Rolph*, 2003]. The lower left graph shows a plot of the inverse NO_3 lifetime, $\tau_{NO_3}^{-1}$, against the unitless quantity $K_{eq}[NO_2]$ according to equation (5) for the period of the night during which there were NO_2 data available (the NO_2 chemiluminescence instrument came on line at approximately 4:00 UTC). The slope of the plot gives $k_{N_2O_5} = (5.0 \pm 0.1)\times10^{-4}$ s^{-1}, and the intercept gives $k_{NO_3} = (6.4 \pm 1.2) \times10^{-4}$ s^{-1}. The errors are from the fit alone and are underestimates of the true uncertainties in the derived rate coefficients. In particular, the value of k_{NO_3} obtained from the intercept is not well determined. It is comparable to the average, calculated value, $k_{NO_3}^{Calc}$, from the sum of the measured VOC data, $k_{NO_3}^{Calc} = 1 \times 10^{-3}$ s^{-1} over the same time period. Changing the intercept to the value of $k_{NO_3}^{Calc}$ reduces the slope, i.e. the determined value of $k_{N_2O_5}$, by only 5%. Combined with the measured aerosol surface area of 260 ± 140 μm^2 cm^{-3}

(where the error is from the variability rather than the measurement uncertainty), the value for $k_{N_2O_5}$ yields $\gamma(N_2O_5) = 0.03 \pm 0.02$.

Figure 6 shows a breakdown of the individual contributions to the NO_3 and N_2O_5 sinks for the data in Figure 5 from 4:00 – 9:30 UTC from a plot of the calculated, inverse NO_3 lifetime, $\left(\tau_{NO_3}^{calc}\right)^{-1} = k_{NO_3}^{Calc} + k_{N_2O_5}^{Calc} K_{eq}[NO_2]$. There are four terms that encompass the majority of the NO_3 and N_2O_5 losses: N_2O_5 hydrolysis (weighted by $K_{eq}[NO_2]$ and with $\gamma(N_2O_5) = 0.03$), NO_3 reactions with terrestrially-emitted biogenic VOC, NO_3 reaction with DMS, and NO_3 reaction with anthropogenic VOC. The solid red line shows the comparison to $\tau_{NO_3}^{-1} = k_1[NO_2][O_3]/[NO_3]$. The pie chart in the inset shows the average, relative contributions of each component of the NO_3 and N_2O_5 losses. Hydrolysis of N_2O_5 was the dominant loss pathway (82%) because of the relatively large mixing ratios of NO_2, which weights the loss in favor of N_2O_5, and because of the small loading of biogenic VOC, particularly DMS. Of the remaining 18% attributable to NO_3 reactions, the largest contribution was reaction with terrestrial biogenic VOC – i.e., biogenic VOC that was emitted from sources over land and advected out into the marine boundary layer, primarily isoprene and monoterpenes (e.g. α-pinene). Anthropogenic compounds, though they were abundant in this environment, are in general not particularly reactive with NO_3 and thus were calculated to have contributed only 4% to the loss. The calculated contribution of dimethyl sulfide to NO_3 and N_2O_5 loss on July 29-30 was anomalously low at only 2% because of small DMS concentrations, while heterogeneous loss of NO_3 would be predicted to contribute an additional 2% based on the assumed $\gamma(NO_3)$ given above. A larger $\gamma(NO_3)$ would obviously yield a larger contribution from heterogeneous loss; however, the small determined value of $k_{NO_3}^{Obs}$ for the single night shown in Figure 5 suggests that $\gamma(NO_3)$ was not likely to be much larger than its literature value on this night. This partitioning of losses yields a value of S in equations (11-12) of 1.82 averaged over the entire night. Therefore, the total loss of NO_x should have proceeded at nearly twice the rate of the $NO_2 + O_3$ reaction.

Figure 7 shows a similar set of data and analysis for August 2-3, 2002. The R/V *Brown* was just north of Cape Anne (northern Massachusetts coast) under conditions of SW to W flow. This night was similar to that in Figure 5 in that the NO_3 sinks were

small and the observed and calculated lifetimes were in reasonable agreement. The plot of $\tau_{NO_3}^{-1}$ vs. $K_{eq}[NO_2]$ shown in the lower right graph also gives a similar result to the night of July 29-30, although the scatter in these data make it more difficult to determine $k_{N_2O_5}$. A fit with the intercept constrained to the calculated value of $k_{NO_3}^{Calc}$=5.6×10^{-4} s^{-1} gives a slope of $k_{N_2O_5}$ = 6.1×10^{-4} s^{-1}, while an unconstrained fit gives $k_{N_2O_5}$ = 4.7×10^{-4} s^{-1} and a larger intercept. Taking the average of the two fits gives $k_{N_2O_5}$ = (5.4 ± 0.7)×10^{-4} s^{-1}. The solid line shows the constrained fit, and the text on the graph shows the inverse of the first order N_2O_5 loss rate coefficient in minutes. Combined with the surface area value over this time period of 180 ± 30 μm^2 cm^{-3}, the derived N_2O_5 uptake coefficient is $\gamma(N_2O_5)$ = 0.04 ± 0.01, consistent with the preceding example. Figure 8 shows the time series of the sum of the calculated losses and a pie chart of the averages for the entire night. Compared to July 29-30, the reaction with DMS accounted for a larger fraction of the NO_3 loss (10%), while terrestrial biogenic VOC (isoprene, monoterpenes) reactions with NO_3 were negligible (2%). Similar to July 30th, however, loss of N_2O_5 accounted for 80% of the total, the value of S in equation (11) was 1.80, and the NO_x loss rate was nearly twice the rate of reaction (1).

Table I summarizes the data for N_2O_5 first order loss rate coefficients for the two nights discussed above. The first three columns show the first order N_2O_5 loss rate coefficient, the aerosol surface area and the uptake coefficients, $\gamma(N_2O_5)$. The derived uptake coefficients are in the same range as literature values for N_2O_5 uptake on sulfate and ammonium sulfate aerosols from laboratory measurements [*Hallquist, et al.*, 2003; *Hu and Abbatt*, 1997; *Kane, et al.*, 2001; *Mentel, et al.*, 1999]. The aerosol composition during NEAQS 2002 was dominated by organics (41-68%) and, ammonium sulfate ($(NH4)_yH_xSO_4$) (23-54%). The $(NH4)_yH_xSO_4$ fraction tended to be acidic, with a mean ammonium to sulfate molar ratio of 1.7[*Bates et al., 2005*]. Laboratory studies with organic and/or mixed organic/inorganic aerosol have shown significantly smaller values of $\gamma(N_2O_5)$ in some cases relative to pure inorganic substrates [*Thornton et al., 2003; Folkers et al., 2003*]. A more recent field study using aircraft data has shown strong suppression of $\gamma(N_2O_5)$ in some air masses that appeared to have been related to the aerosol organic fraction or to the aerosol acidity [*Brown et al., 2006*]. In the NEAQS

2002 study, the data were not of sufficient quality for a systematic determination of the dependence of $\gamma(N_2O_5)$ on aerosol composition.

The above analysis was based on the assumption that the hydrolysis of N_2O_5 proceeds exclusively via heterogeneous uptake on aerosol. Wahner and coworkers [*Mentel, et al.*, 1996; *Wahner, et al.*, 1998] have measured rate coefficients for a homogeneous gas-phase component for N_2O_5 hydrolysis based on their data from large chamber studies. They found the proposed reaction to be the sum of a first and second order component in water vapor.

$$k_{homogeneous}(N_2O_5) = k_I \times [H_2O] + k_{II} \times [H_2O]^2 \quad (13)$$

$$k_I = 2.5 \times 10^{-22} \text{ cm}^3 \text{ molecule}^{-1} \text{ s}^{-1}$$

$$k_{II} = 1.8 \times 10^{-39} \text{ cm}^6 \text{ molecule}^{-2} \text{ s}^{-1}$$

Columns 5 and 6 in Table I give the N_2O_5 loss rate coefficients for each component of the homogeneous loss rate coefficient in equation (13). For July 30th and August 3rd, the first order component would modestly reduce the uptake coefficients but would still allow for heterogeneous reaction to occur. Inclusion of the second order component in equation (13) would require that essentially all of the N_2O_5 loss was due to the homogeneous reaction. Because of the considerable uncertainty in the field determinations of N_2O_5 first order loss rate coefficients from the NEAQS 2002 data, it is not possible to rule out the parameterization of the homogeneous N_2O_5 hydrolysis shown above. However, given that heterogeneous hydrolysis is known to occur, the N_2O_5 loss rate coefficients derived form this field data set suggest that the smog-chamber parameterization of the homogeneous hydrolysis is larger than this determination from ambient field data would support. This conclusion holds true for all of the NO_3 and N_2O_5 data from the NEAQS 2002 campaign and is also supported by an analysis of a more recent data set acquired from an aircraft [*Brown, et al.*, 2006].

5.2 Case 2: Losses Dominated by NO_3 reactions

There were several nights during the 2002 campaign on which there were large mixing ratios of biogenic VOC, and, consequently, large losses of NO_3 in comparison to those for N_2O_5. Figure 9 illustrates such a case. The R/V *Brown* was again off of the northern Massachusetts coast under conditions of offshore flow (SW wind early in the night, NW flow later). The average of the total losses for NO_3 and N_2O_5 on this night were significantly larger than those in Figs. 6 and 8, mainly due to the presence of isoprene, monoterpenes (the terrestrially emitted biogenic VOC) and DMS. The aerosol surface, and therefore the predicted N_2O_5 heterogeneous loss rate constant, were similar to the previous two examples, but in this case were smaller than the calculated VOC loss rates. Because of the rapid loss rates, NO_3 and N_2O_5 were only observed during two distinct, large NO_2 plumes, one early and one late in the night, as marked in the figure.

The decrease in the calculated loss rates for NO_3 that were associated with each plume were due to a drop in the mixing ratio of isoprene and monoterpenes within the NO_x-containing plumes. This observation implies that the increased source strength of NO_3 due to the presence of anthropogenic NO_2 increased the nocturnal oxidation rate of biogenic VOC relative to background air – i.e., wherever there was sufficient NO_x to drive VOC oxidation during the transit time to the R/V *Brown*, the VOC concentrations were depleted. This spatial inhomogeneity in the nocturnal oxidation of VOC stands in contrast to daytime oxidation by OH, whose photochemical source from ozone photolysis in the presence of water vapor is more constant and diffusely distributed. At night, nocturnal processing tends to occur most strongly within NO_x-containing plumes. Indeed, the second plume in Figure 9 was likely from a power plant source (NO_2 was correlated with ~ 15 ppbv of SO_2 in this plume) which emits a large amount of NO_x into a relatively confined region, especially at night when mixing processes are slower.

There was also a lack of agreement between the observed and calculated NO_3 loss rate coefficients for the data in Figure 9. This may be an indication of secondary chemistry occurring subsequent to the initial oxidation step for compounds such as isoprene and DMS, either as a result of peroxy radical reactions [*Carslaw, et al.*, 1997; *Geyer, et al.*, 2003; *Jensen, et al.*, 1992; *Platt, et al.*, 2002; *Platt, et al.*, 1990; *Salisbury,*

et al., 2001] or reactions of NO_3 with secondary oxidation products (e.g., organic nitrates) [*Atkinson and Arey*, 2003], neither of which was measured during this campaign. Although it is not possible to quantify the potential contribution of these additional NO_3 reactions from the existing measurements, future modeling studies of this and other data sets will address these issues.

A second example of large NO_3 losses due to the presence of biogenic VOC appears in Figure 10, which shows NO_3 and N_2O_5 mixing ratios for the night of July 30-31, 2002. On this night the R/V *Brown* was outside of Boston Harbor, south of Cape Anne and made SW-NE running transects perpendicular to a NW wind. Back trajectories showed relatively rapid transport (within a few hours) from central NH, an area with significant monoterpene emission [*Geron, et al.*, 1994]. The figure demonstrates the interaction that can occur between different VOCs as a result of their common loss due to NO_3. The observed mixing ratio of the pinenes was anticorrelated with NO_3, as would be expected and as has been described previously by [*Warneke, et al.*, 2004]. As described in the preceding example, the anticorrelation is presumably the result of loss of the reactive pinenes during transport to the R/V *Brown* in air masses impacted by NO_2 emissions with increased source strength for NO_3 (observed on the SW end of each transect as the *Brown* sampled downwind of the Boston area). For example, the lifetime of α-pinene with respect to NO_3 oxidation averaged 8 minutes from 5:00 - 6:00 UTC when it was not observed, and >5 hours from 3:00 – 4:30 UTC, when it was present. During the latter part of the time series, the concentrations of pinenes and DMS were well correlated, even though DMS arises from an ocean source and the pinenes from a terrestrial one. In the air masses with lower NO_2 and measurable pinene mixing ratios, the increased concentrations of DMS were likely a result not only of decreased oxidation rate due to smaller NO_3 source strength (i.e., a smaller amount of available NO_3), but also of competition between the monoterpenes and DMS for the available NO_3. For example, α-pinene reacts with NO_3 approximately 6× faster than does DMS [*Atkinson*, 1991], and so can effectively suppress nocturnal, NO_3-driven oxidation of DMS when it is present. The example demonstrates the interaction between the terrestrially emitted biogenic VOC and DMS in a polluted environment via their common sink to NO_3 reaction, and shows

that DMS oxidation at night can be influenced not just by the presence of NO_3 derived from NO_x, but also by other VOCs that act as sinks for NO_3.

5.3 Case 3: Weak Sinks for NO_3 and N_2O_5

Although the observed lifetimes of NO_3 and N_2O_5 were quite short (i.e., on the order of a few minutes for NO_3) throughout the measurement period within the Gulf of Maine, the same was not true of other regions sampled during NEAQS 2002. Figure 11 shows the time series of NO_3, N_2O_5 and NO_2 from August 7-8, 2002, when the R/V *Brown* was well south of the New England study area on the transit back to its home port in Charleston, SC. Observed lifetimes of NO_3 and N_2O_5 in this region were considerably longer (e.g., in excess of 30 minutes for NO_3). The map in the lower corner shows the R/V *Brown* position and back trajectories showing that the sampled air mass came from the north, passing over the New York City area roughly 12-14 hours upwind. There was somewhat lower NO_x (~1.5 ppbv NO_2) compared to most of the air sampled in the New England region that was of continental origin, yet the NO_3 mixing ratio reached its largest sustained values of the entire campaign (> 100 pptv). Mixing ratios of N_2O_5 reached by far their largest observed values under similar conditions on the following night (see Figure 3) near Norfolk, VA. The inverse NO_3 lifetime, $\tau_{NO_3}^{-1}$, in the center panel shows reasonable agreement with the calculated loss rate coefficients, $k_{NO_3}^{Calc}$, although the value for $\gamma(N_2O_5) = 0.03$, determined under conditions of rapid N_2O_5 loss in the Gulf of Maine, may have been an overestimate in this region (see below). The apparent disagreement between the observed and calculated NO_3 lifetimes early in the night, until approximately 3:30 UTC, is in fact not due to a disagreement between the steady-state model and the measurements. Rather, this is a case in which the approach to steady state was limited by the induction time (i.e., the time constant for loss of NO_3 and N_2O_5) [*Allan, et al.*, 2000] due to the apparently weak sinks within this air mass. The disagreement late in the night, on the other hand, was likely due to a shift to a different air mass in which the sinks for NO_3 and N_2O_5 were not well accounted for. The slow losses for NO_3 and N_2O_5 may have been the result of a number of factors. First, the mixing ratios of biogenic VOCs were small; terrestrially emitted biogenic VOC were all below their instrumental detection

limits (< 1 pptv), and DMS was observed at a maximum of 20 pptv prior to sunset. The aerosol surface area density was also relatively small, with an average value of 130 μm^2 cm^{-3}. Another factor that was distinct on the night of August 7-8 was the relative humidity of 55%, the smallest nocturnal average value of the campaign. Platt *et al.*[1984], for example, have reported large increases in NO_3 and N_2O_5 lifetimes at low RH over desert regions of southern California that they attributed to decreased aerosol particle growth. A final difference on August 7-8 was the depth of the mixed layer, which radiosonde data showed to be deeper on this leg of the R/V *Brown* cruise (~1 km) than in the Gulf of Maine (100 km).[*Angevine, et al.*, 2004] The deeper mixed layer may in turn have been related to warmer sea surface temperatures (25 °C compared to 18°C in the Gulf of Maine) and may, among other things, have served to reduce the concentration of sinks for NO_3 and N_2O_5, such as DMS emitted from the ocean surface. In any case, Figure 11 shows that NO_3 and N_2O_5 losses were not observed to be universally rapid within the marine boundary layer during NEAQS 2002, and furthermore, that the variation in observed lifetimes may have been related to regional differences in factors such as DMS emissions, sea surface temperature and boundary layer mixing. We intend to explore these issues further in a forthcoming campaign in the Gulf of Mexico.

5.4 Summary of Losses for the entire campaign

Figure 12 shows a summary of the losses for NO_3 and N_2O_5 for the duration of the campaign. The averages in the chart are the calculated losses for nighttime hours only, and only for the time periods where NO_3 and N_2O_5 were reported. Direct losses for NO_3 were dominated by reactions with VOC, with heterogeneous uptake using the literature value of $\gamma(NO_3) = 4\times10^{-3}$ contributing only 2% to the total. Of the VOC losses, DMS was the most important, followed by terrestrially emitted biogenic hydrocarbons (mostly isoprene and monoterpenes). Only a small fraction of the total (7%) could be attributed to NO_3 reaction with anthropogenic VOC. The N_2O_5 loss is calculated using the measured aerosol surface area and a constant $\gamma(N_2O_5) = 0.03$, as determined from the analysis in section 5.1. Assuming this uptake coefficient is representative of the entire data set, the individual losses for NO_3 and N_2O_5, were, on average, approximately equal

contributions to the total loss of the pair. Since the lifetime of these compounds were short enough to make reaction (1) the rate limiting step for loss of NO_x at night, the average value of S in equation (11-12) for this campaign should have been approximately 1.5 – i.e., the loss of NO_x at night occurred, on average, at 1.5 times the rate of the reaction of NO_2 with O_3. At the campaign average nocturnal O_3 concentration of 41 ppbv, the calculated nocturnal lifetime of NO_x (i.e., $(Sk_1[O_3])^{-1}$) was 6.0 hours, corresponding to greater than 80% loss of NO_x in a 10 hour night.

6. Nocturnal Halogen Activation

Uptake of both NO_3 and N_2O_5 on sea salt aerosol can lead to the release of active halogens compounds to the gas phase according to the following reactions [*Finlayson-Pitts, et al.*, 1989; *Rossi*, 2003].

$$N_2O_5\ (g) + NaX\ (aq) \rightarrow XNO_2\ (g) + NaNO_3\ (aq) \qquad (14)$$

$$NO_3\ (g) + NaX\ (aq) \rightarrow X\ (g) + NaNO_3\ (aq) \qquad (15)$$

Here, X is primarily Cl but may include a small amount of Br [*Behnke, et al.*, 1994]. This chemistry is potentially important in marine environments since halogen atoms are potent oxidants, and since they can participate in cycles that catalytically remove ozone [*Finlayson-Pitts, et al.*, 1989]. Aside from HCl, there were no measurements of gas phase halogens or halogen compounds as part of the R/V *Brown* measurement suite. The largest source of HCl in this polluted marine environment was most likely the uptake of nitric and/or sulfuric acid on sea salt. Thus, there is no direct observational evidence for reactions (14 - 15) from the NEAQS 2002 campaign.

The nocturnal reactive halogen source may nevertheless be estimated from the measured sea salt abundance, the concentrations of NO_3 and N_2O_5, and the uptake coefficients for these compounds on sea salt from laboratory studies. The aerosol surface area attributable to sea salt can be calculated from the aerosol size distributions in the supermicron range, which were dominated by sea salt and NO_3^- . Submicron aerosol, by contrast, was dominated by NH_4^+, non sea-salt sulfate and organics [*Bates, et al.*, 2005].

The average calculated sea salt surface area density during NEAQS 2002 was small, at 5.5 μm^2 cm^{-3}, or about 2% of the total aerosol surface, consistent with low wind speeds (avg. $\pm$ 1σ = 5 $\pm$ 2 m s^{-1}) in the Gulf of Maine in summer. A typical value for the uptake coefficient of N_2O_5 on aqueous salt solutions from lab studies is 0.03 [*Behnke, et al.*, 1997; *Stewart, et al.*, 2004], and the calculated N_2O_5 uptake rate on sea salt varied from zero up to 4×10^4 molecules cm^{-3} s^{-1}. The night of August 2-3 (see Figs. 7-8) showed the strongest sustained uptake rates, with an average value of 3×10^4 molecules cm^{-3} s^{-1}, as shown in Figure 13. The yield and the fate of the resulting $ClNO_2$ product is unknown. Assuming that it survives until sunrise, when it can be photolyzed to release Cl, the integrated halogen production on August 2-3 would have amounted to a 45 pptv reservoir, as shown against the right axis of Figure 13. Similarly, uptake coefficients for NO_3 on sea salt are in the range $\gamma(NO_3)_{SS}$ = 1-6 $\times$ 10^{-3} [*Rudich, et al.*, 1996]. Taking the 6×10^{-3} as an upper limit, the calculated uptake rates for NO_3 on sea salt vary between 0 - 6×10^3 molecules cm^{-3} s^{-1}. Figure 13 shows the Cl production rate and integrated Cl yield for NO_3 on August 2-3 assuming unit yield and no loss. It is important to stress that these estimates represent upper limits from the night with the strongest predicted source.

There is insufficient evidence available from our analysis of this data set to date to test a halogen source of this magnitude at sunrise. Hydrocarbon oxidation, for example, was observed to proceed rapidly during the night and day, but much more slowly during the dawn and dusk periods [*Warneke, et al.*, 2004]. The release of a halogen reservoir at dawn from photolysis of, for example, $ClNO_2$ with a lifetime of 1 hour [*Behnke, et al.*, 1997], would tend to introduce faster VOC oxidation rates at this time of day, contrary to what was observed. Even though a dawn source rate for active Cl of the order of 3×10^5 atoms cm^{-3} s^{-1} is substantial, the integrated effect on the oxidation of VOC would be modest. Thus, the nocturnal halogen production cannot be easily quantified on the basis of the available data.

7. Summary & Conclusion

Ship-based, *in-situ* measurements of NO_3 and N_2O_5 in the polluted marine boundary layer off of the United States East Coast during the summer of 2002 from the

NOAA research vessel *Ronald H. Brown* give a detailed picture of the nocturnal chemistry that governs both the rate of NO_x loss and the oxidation of VOC. Steady-state lifetimes for NO_3 and N_2O_5 were comparable to those determined from previous surface-level DOAS measurements of NO_3. Analysis of the dependence of steady state lifetimes on NO_x, combined with calculated loss rate coefficients from measured aerosol loading and VOC concentrations allows for an accounting of the individual contributions to the losses of NO_3 and N_2O_5, and in some cases an estimate for the uptake coefficients for heterogeneous hydrolysis of N_2O_5, $\gamma(N_2O_5)$. Heterogeneous uptake coefficients determined from this data set were $\gamma(N_2O_5) = 0.03 \pm 0.02$ and compare well with literature values from laboratory measurements. The most obvious discrepancies between the observed and calculated NO_3 and N_2O_5 lifetimes occurred either on nights with large concentrations of biogenic VOC (isoprene, monoterpenes, DMS), possibly as a result of secondary chemistry between NO_3 and unmeasured second-generation reaction products. For the campaign as a whole, the loss partitioning between NO_3 and N_2O_5 was approximately equal - i.e., about 50% of the loss of the NO_3 and N_2O_5 pair was due to reactions of each compound. Because NO_3 and N_2O_5 loss was rapid on most nights and because N_2O_5 hydrolysis was predicted to be responsible for roughly half of this loss, the removal of anthropogenic NO_x in this polluted marine environment was rate limited by the reaction of NO_2 with O_3 and proceeded at approximately 1.5 × the rate of this reaction. Finally, halogen chemistry arising from the displacement of halides from sea salt aerosol by NO_3 and N_2O_5 may have provided a dawn Cl source during NEAQS 2002, but there are insufficient data available to test the magnitude of this source.

8. Acknowledgements

We thank the crew of the NOAA R/V *Ronald H. Brown*. Dr. Wayne Angevine provided analysis of radiosonde data for determination of marine boundary layer mixing depths. This work was funded by NOAA's Air Quality Program and the New England Air Quality Study.

References

Allan, B. J., N. Carslaw, H. Coe, R. A. Burgess, and J. M. C. Plane (1999), Observations of the Nitrate Radical in the Marine Boundary Layer, *J. Atmos. Chem.*, *33*, 129-154.

Allan, B. J., G. McFiggans, J. M. C. Plane, H. Coe, and G. G. McFadyen (2000), The nitrate radical in the remote marine boundary layer, *J. Geophys. Res.*, *105*, 24,191-124,204.

Angevine, W. M., C. J. Senff, A. B. White, E. J. Williams, J. Koermer, S. T. K. Miller, R. Talbot, P. E. Johnston, S. A. McKeen, and T. Downs (2004), Coastal Boundary Layer Influence on Pollutant Transport in New England, *J. Appl. Meteor.*, *43*, 1425-1437.

Atkinson, R. (1991), Kinetics and Mechanism of the Gas-Phase Reactions of the NO_3 Radical with Organic Compounds, *J. Phys. Chem. Ref. Data*, *20*, 459-507.

Atkinson, R., and J. Arey (2003), Atmospheric Degradation of Volatile Organic Compounds, *Chem. Rev.*, *103*, 4605-4638.

Bates, T. S., P. K. Quinn, D. J. Coffman, J. E. Johnson, and A. M. Middlebrook (2005), Dominance of organic aerosols in the marine boundary layer over the Gulf of Maine during NEAQS 2002 and their role in aerosol light scattering, *J. Geophys. Res.*, *110*, D18202, doi:18210.11029/12005JD005797.

Behnke, W., C. George, V. Scheer, and C. Zetzsch (1997), Production and decay of $ClNO_2$ from the reaction of gaseous N_2O_5 with NaCl solution: Bulk and aerosol experiments, *J. Geophys. Res.*, *102*, 3795-3804.

Behnke, W., V. Scheer, and C. Zetzsch (1994), Production of $BrNO_2$, Br_2 and $ClNO_2$ from the reaction between sea spray aerosol and N_2O_5., *J. Aerosol Sci.*, *25*, S277-S278.

Brown, S. S., J. E. Dibb, H. Stark, M. Aldener, M. Vozella, S. Whitlow, E. J. Williams, B. M. Lerner, R. Jakoubek, A. M. Middlebrook, J. A. DeGouw, C. Warneke, P. D. Goldan, W. C. Kuster, W. M. Angevine, D. T. Sueper, P. K. Quinn, T. S. Bates, J. F. Meagher, F. C. Fehsenfeld, and R. A. R. (2004), Nighttime removal of NO_x in the summer marine boundary layer, *Geophys. Res. Lett.*, *31*, L07108, doi:07110.01029/02004GL019412.

Brown, S. S., T. B. Ryerson, A. G. Wollny, C. A. Brock, R. Peltier, A. P. Sullivan, R. J. Weber, J. S. Holloway, W. P. Dubé, M. Trainer, J. F. Meagher, F. C. Fehsenfeld, and A. R. Ravishankara (2006), Variability in nocturnal nitrogen oxide processing and its role in regional air quality, *Science*, *311*, 67-70.

Brown, S. S., H. Stark, S. J. Ciciora, R. J. McLaughlin, and A. R. Ravishankara (2002), Simultaneous in-situ detection of atmospheric NO_3 and N_2O_5 via cavity ring-down spectroscopy, *Rev. Sci. Instr.*, *73*, 3291-3301.

Brown, S. S., H. Stark, and A. R. Ravishankara (2003), Applicability of the Steady-State Approximation to the Interpretation of Atmospheric Observations of NO_3 and N_2O_5, *J. Geophys. Res.*, *108*, D174539, doi:174510.171029/172003JD003407.

Busch, K. W., and M. A. Busch (Eds.) (1999), *Cavity-Ringdown Spectroscopy*, American Chemical Society, Washington, DC.

Carslaw, N., L. J. Carpenter, J. M. C. Plane, B. J. Allan, R. A. Burgess, K. C. Clemitshaw, H. Coe, and S. A. Penkett (1997), Simultaneous observations of nitrate and peroxy radicals in the marine boundary layer, *J. Geophys. Res.*, *102*, 18917-18933.

Dentener, F. J., and P. J. Crutzen (1993), Reaction of N_2O_5 on Tropospheric Aerosols: Impact on the Global Distributions of NO_x, O_3, and OH, *J. Geophys. Res.*, *98*, 7149-7163.

Dibb, J. E., E. Scheuer, S. I. Whitlow, M. Vozella, E. Williams, and B. M. Lerner (2004), Ship-based nitric acid measurements in the Gulf of Maine during New England Air Quality Study 2002, *J. Geophys. Res.*, *109*, D20303, doi:20310.21029/22004JD004843.

Draxler, R. R., and G. D. Rolph (2003), HYSPLIT (HYbrid Sinlge-Particle Lagrangian Integrated Tracker) Model access via NOAA ARL Ready Website (http://www.arl.noaa.gov/ready/hysplit4.html), edited, NOAA Air Resources Laboratory, Silver Spring, MD.

Dubé, W. P., S. S. Brown, H. D. Osthoff, M. R. Nunley, S. J. Ciciora, M. W. Paris, R. J. McLaughlin, and A. R. Ravishankara (2006), An aircraft instrument for simultaneous, in-situ measurements of NO_3 and N_2O_5 via cavity ring-down spectroscopy, *Rev. Sci. Instr.*, *77*, 034101.

Finlayson-Pitts, B. J., M. J. Ezell, and J. N. J. Pitts (1989), Formation of chemically active chlorine compounds by reactions of atmospheric NaCl particles with gaseous N_2O_5 and $ClONO_2$, *Nature*, *337*, 241-244.

Fuchs, N. A., and A. G. Stugnin (1970), *Highly Dispersed Aersols*, Ann Arbor Science, Ann Arbor, MI.

Geron, C. D., A. B. Guenther, and T. E. Pierce (1994), An improved model for estimating emissions of volatile organic compounds from forests in the eastern United States, *J. Geophys. Res.*, *00*, 12,773-712,791.

Geyer, A., R. Ackermann, R. Dubois, B. Lohrmann, R. Müller, and U. Platt (2001), Long-term observation of nitrate radicals in the continental boundary layer near Berlin, *Atmos. Environ.*, *35*, 3619-3631.

Geyer, A., K. Bachmann, A. Hofzumahaus, F. Holland, S. Konrad, T. Klupfel, H. W. Patz, D. Perner, D. Mihelcic, H. J. Schafer, A. Volz-Thomas, and U. Platt (2003), Nighttime formation of peroxy and hydroxyl radicals during the BERLIOZ campaign: Observations and modeling studies, *J. Geophys. Res.*, *108*, D48249, doi: 48210.41029/42001JD000656.

Geyer, A., and J. Stutz (2004), Vertical profiles of NO_3, N_2O_5, O_3, and NO_x in the nocturnal boundary layer: 2. Model studies on the altitude dependence of composition and chemistry, *J. Geophys. Res.*, *109*, D12307, doi: 12310.11029/12003JD004211.

Goldan, P. D., W. C. KusterE, E. Williams, P. C. Murphy, F. C. Fehsenfeld, and J. Meagher (2004), Nonmethane hydrocarbon and oxy hydrocarbon measurements during the 2002 New England Air Quality Study, *J. Geophys. Res.*, *109*, D21309, doi:21310.21029/22003JD004455.

Hallquist, M., D. J. Stewart, S. K. Stephenson, and R. A. Cox (2003), Hydrolysis of N_2O_5 on sub-micron sulfate aerosols, *Phys. Chem. Chem. Phys.*, *5*, 3453-3463.

Heintz, F., U. Platt, J. Flentje, and R. Dubois (1996), Long-term observation of nitrate radicals at the Tor Station, Kap Arkona (Rügen), *J. Geophys. Res.*, *101*, 22891-22910.

Hu, J. H., and J. P. D. Abbatt (1997), Reaction probabilities for N_2O_5 hydrolysis on sulfuric acid and ammonium sulfate aerosols at room temperature, *J. Phys. Chem. A.*, *101*, 871-878.

Jensen, N. R., J. Hjorth, C. Lohse, H. Skov, and G. Restelli (1992), Products and Mechanisms of the Gas Phase Reactions of NO_3 with CH_3SCH_3, CD_3SCD_3, CH_3SH and CH_3SSCH_3, *J. Atmos. Chem.*, *14*, 95-108.

Kane, S. M., F. Caloz, and M.-T. Leu (2001), Heterogeneous Uptake of Gaseous N_2O_5 by $(NH_4)_2SO_4$, NH_4SO_4, and H_2SO_4 Aerosols, *J. Phys. Chem. A.*, *105*, 6465-6470.

Lucas, D. D., and R. G. Prinn (2005), Parametric sensitivity and uncertainty analysis of dimethylsulfide oxidation in the clear-sky remote marine boundary layer, *Atmos. Chem. Phys.*, *5*, 1505-1525.

Martinez, M., D. Perner, E.-M. Hackenthal, S. Külzer, and L. Schültz (2000), NO_3 at Helgoland during the NORDEX campaign in October 1996, *J. Geophys. Res.*, *105*, 22685-22695.

Mentel, T. F., D. Bleilebens, and A. Wahner (1996), A study of nighttime nitrogen oxide oxidation in a large reaction chamber - The fate of NO_2 N_2O_5, HNO_3, and O_3 at different humidities, *Atmospheric Environment*, *30*, 4007-4020.

Mentel, T. F., M. Sohn, and A. Wahner (1999), Nitrate effect in the heterogeneous hydrolysis of dinitrogen pentoxide on aqueous aerosols, *Physical Chemistry Chemical Physics*, *1*, 5451-5457.

Moldanova, J., and E. Ljungstrom (2000), Modelling of particle formation from NO_3 oxidation of selected monoterpenes, *Journal of Aerosol Science*, *31*, 1317-1333.

Platt, U., B. Alicke, R. Dubois, A. Geyer, A. Hofzumahaus, F. Holland, M. Martinez, D. Mihelcic, T. Klüpfel, B. Lohrmann, W. Pätz, D. Perner, F. Rohrer, J. Schäfer, and J. Stutz (2002), Free Radicals and Fast Photochemistry during BERLIOZ, *J. Atmos. Chem.*, *42*, 359-394.

Platt, U., and F. Heintz (1994), Nitrate Radicals in Tropospheric Chemistry, *Israel J. of Chem.*, *34*, 289-300.

Platt, U., G. LeBras, G. Poulet, J. P. Burrows, and G. Moortgat (1990), Peroxy radicals from night-time reactions of NO_3 with organic compounds, *Nature*, *348*, 147-149.

Platt, U. F., A. M. Winer, H. W. Bierman, R. Atkinson, and J. N. Pitts, Jr. (1984), Measurement of Nitrate Radical Concentrations in Continental Air, *Environ. Sci. Technol.*, *18*, 365-369.

Richards, L. W. (1983), Comments on the oxidation of NO_2 to nitrate - Day and night, *Atmos. Environ.*, *17*, 397-402.

Rossi, M. J. (2003), Heterogeneous Reactions on Salts, *Chem. Rev.*, *103*, 4823-4882.

Rudich, Y., R. K. Talukdar, A. R. Ravishankara, and R. W. Fox (1996), Reactive uptake of NO_3 on pure water and ionic solutions, *J. Geophys. Res.*, *101*, 21,023-021,031.

Salisbury, G., A. R. Rickard, P. S. Monks, B. J. Allan, S. Bauguitte, S. A. Penkett, N. Carslaw, A. C. Lewis, D. J. Creasey, D. E. Heard, P. J. Jacobs, and J. D. Lee (2001), Production of peroxy radicals at night via reactions of ozone and the nitrate radical in the marine boundary layer, *J. Geophys. Res.*, *106*, 12669-12687.

Sander, S. P., R. R. Friedl, D. M. Golden, M. J. Kurylo, R. E. Huie, V. L. Orkin, G. K. Moortgat, A. R. Ravishankara, C. E. Kolb, M. J. Molina, and B. J. Finlayson-Pitts (2003), *Chemical Kinetics and Photochemical Data for Use in Atmospheric Studies*, JPL Publication 02-25, Pasadena, CA.

Smith, N., J. M. C. Plane, C.-F. Nien, and P. A. Solomon (1995), Nighttime radical chemistry in the San Joaquin valley, *Atmos. Environ.*, *29*, 2887-2897.

Stark, H., P. D. Goldan, S. S. Brown, M. Aldener, W. C. Kuster, and A. R. Ravishankara (2006), Influence of the nitrate radical on the oxidation of dimethyl sulfide in a polluted marine environment, *J. Geophys. Res.*, *submitted*.

Stewart, D. J., P. T. Griffiths, and R. A. Cox (2004), Reactive uptake coefficients for heterogeneous reaction of N_2O_5 with submicron aerosols of NaCl and natural sea salt, *Atmos. Chem. Phys.*, *4*, 1381-1388.

Thornton, J. A., P. J. Wooldridge, R. C. Cohen, E. J. Williams, D. Hereid, F. C. Fehsenfeld, J. Stutz, and B. Alicke (2003), Comparisons of in situ and long path measurements of NO_2 in urban plumes, *J. Geophys. Res.*, *108*, D164496, doi: 164410.161029/162003JD003559.

Wahner, A., T. F. Mentel, and M. Sohn (1998), Gas-phase reaction of N_2O_5 with water vapor: Importance of heterogeneous hydrolysis of N_2O_5 and surface desorption of HNO_3 in a large Teflon chamber, *Geophysical Research Letters*, *25*, 2169-2172.

Warneke, C., J. A. de Gouw, P. D. Goldan, W. C. Kuster, E. J. Williams, B. M. Lerner, S. S. Brown, H. Stark, M. Aldener, A. R. Ravishankara, J. M. Roberts, M. Marchewka, S. Bertman, D. T. Sueper, S. A. McKeen, J. F. Meagher, and F. C. Fehsenfeld (2004), Comparison of day and nighttime oxidation of biogenic and anthropogenic VOCs along the New England coast in summer during New Enlgand Air Quality Study 2002, *J. Geophys. Res.*, *109*, D10309, doi:10310.11029/12003JD004424.

Wayne, R. P., I. Barnes, P. Biggs, J. P. Burrows, C. E. Canosa-Mas, J. Hjorth, G. LeBras, G. K. Moortgat, D. Perner, G. Poulet, G. Restelli, and H. Sidebottom (1991), The Nitrate Radical: Physics, Chemistry, and the Atmosphere, *Atmos. Environ.*, *25A*, 1-203.

Wesely, M. L., and B. B. Hicks (2000), A review of the current status of knowledge on dry deposition, *Atmos. Environ.*, *34*, 2261-2282.

Winer, A. M., R. Atkinson, and J. N. J. Pitts (1984), Gaseous Nitrate Radical: Possible Nighttime Atmospheric Sink for Biogenic Organic Compounds, *Science*, *224*, 156-158.

Yvon, S. A., J. M. C. Plane, C.-F. Nien, D. J. Cooper, and E. S. Saltzman (1996), Interaction between nitrogen and sulfur cycles in the polluted marine boundary layer, *J. Geophys. Res.*, *101*, 1379-1386.

Table I: Uptake coefficients for N_2O_5 determined from analysis of field data

Date	$k_{N_2O_5}$ (s^{-1})	Surf Area $\mu m^2\ cm^{-3}$	$\gamma(N_2O_5)$	$k_I[H_2O]$ (s^{-1})	$k_{II}[H_2O]^2$ (s^{-1})	γ (N_2O_5) corrected for $k_I \times [H_2O]$
7/30	5.0×10^{-4}	260 ± 140	0.03	1.4×10^{-4}	5.5×10^{-4}	0.018
8/3	5.2×10^{-4}	180 ± 30	0.04	1.3×10^{-4}	5.2×10^{-4}	0.028

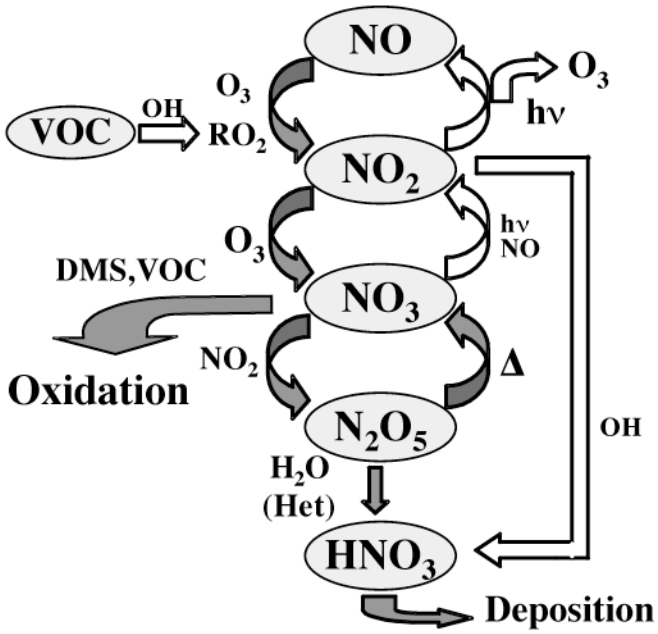

Figure 1. Schematic of nitrogen oxide chemistry showing photochemical ozone production from NO_x (=NO + NO_2) and VOC, conversion of NO_x to the nocturnal nitrogen oxides (=NO_3 + N_2O_5) and their subsequent losses by reactions with VOC and aerosol. Open arrows indicate reactions that take place mainly or exclusively in the presence of sunlight.

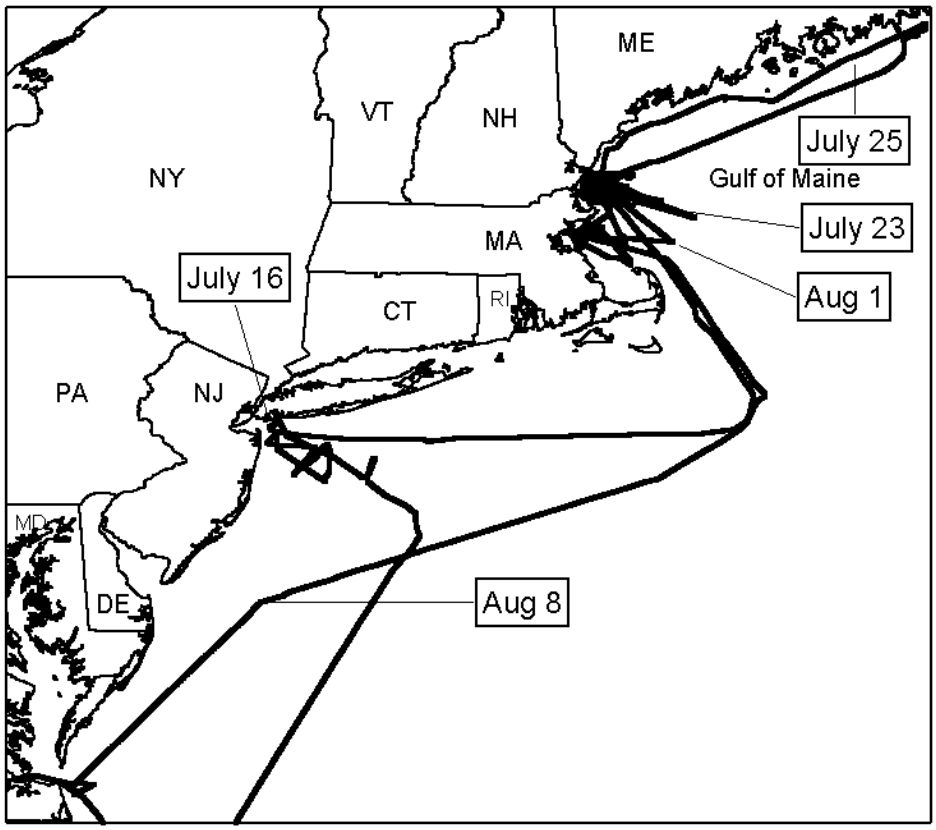

Figure 2. Map of the east coast of the United States showing the track of the R/V *Brown* and the intensive study area in the Gulf of Maine. Selected dates show the location of R/V *Brown* at different points during the campaign.

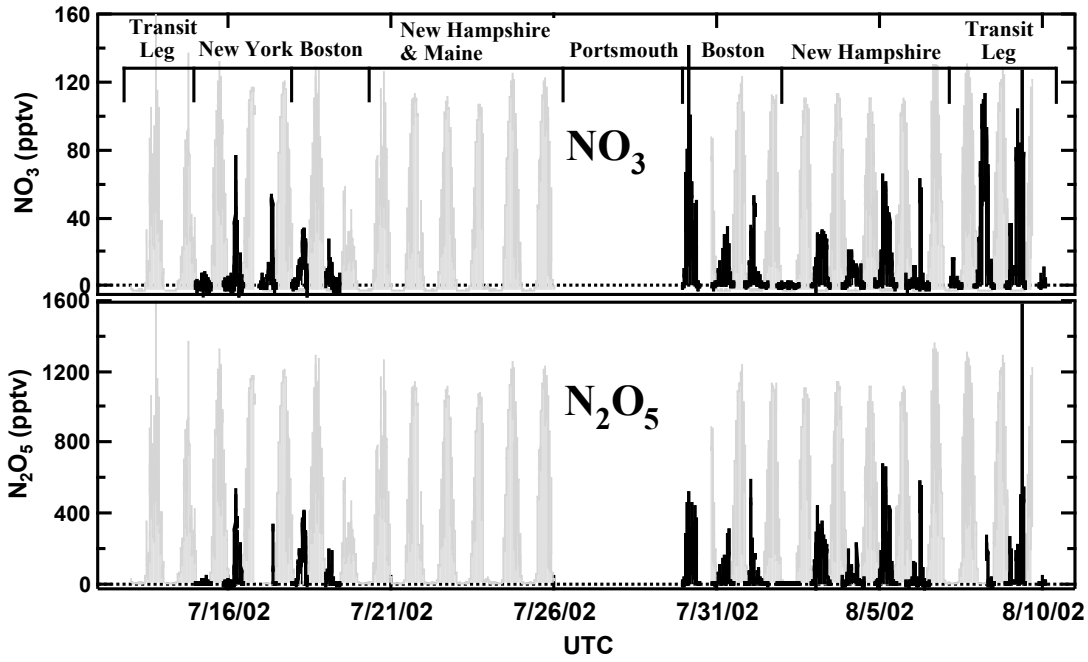

Figure 3. Overview of the measured mixing ratios of NO_3 and N_2O_5. The legend across the top indicates the sampling regions during each period. The gray shaded background shows the solar insolation measured at the ship to give a reference for day vs. night in the time series.

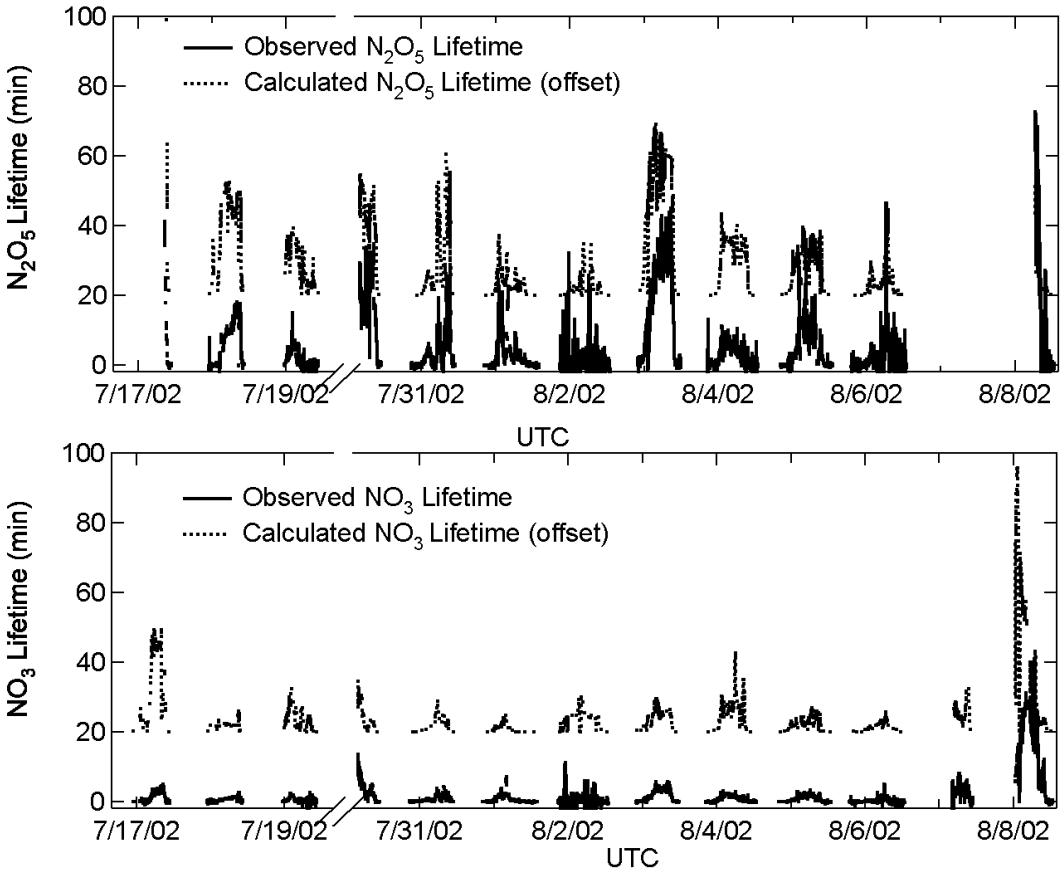

Figure 4. Observed (τ_{NO_3}, $\tau_{N_2O_5}$ from the left hand side of equations 5-6) and calculated ($\tau^{Calc}_{NO_3}, \tau^{Calc}_{N_2O_5}$ from the right hand side of equations 5-6 using $k^{Calc}_{NO_3}, k^{Calc}_{N_2O_5}$ from equations 7, 8 respectively) steady state lifetimes for NO_3 and N_2O_5. Note that the gap in the data from Fig. 3 is omitted from this time series (break in the x-axis). Calculated values have been offset by +20 minutes for clarity (they are overlaid with no offset in the color version of the figure).

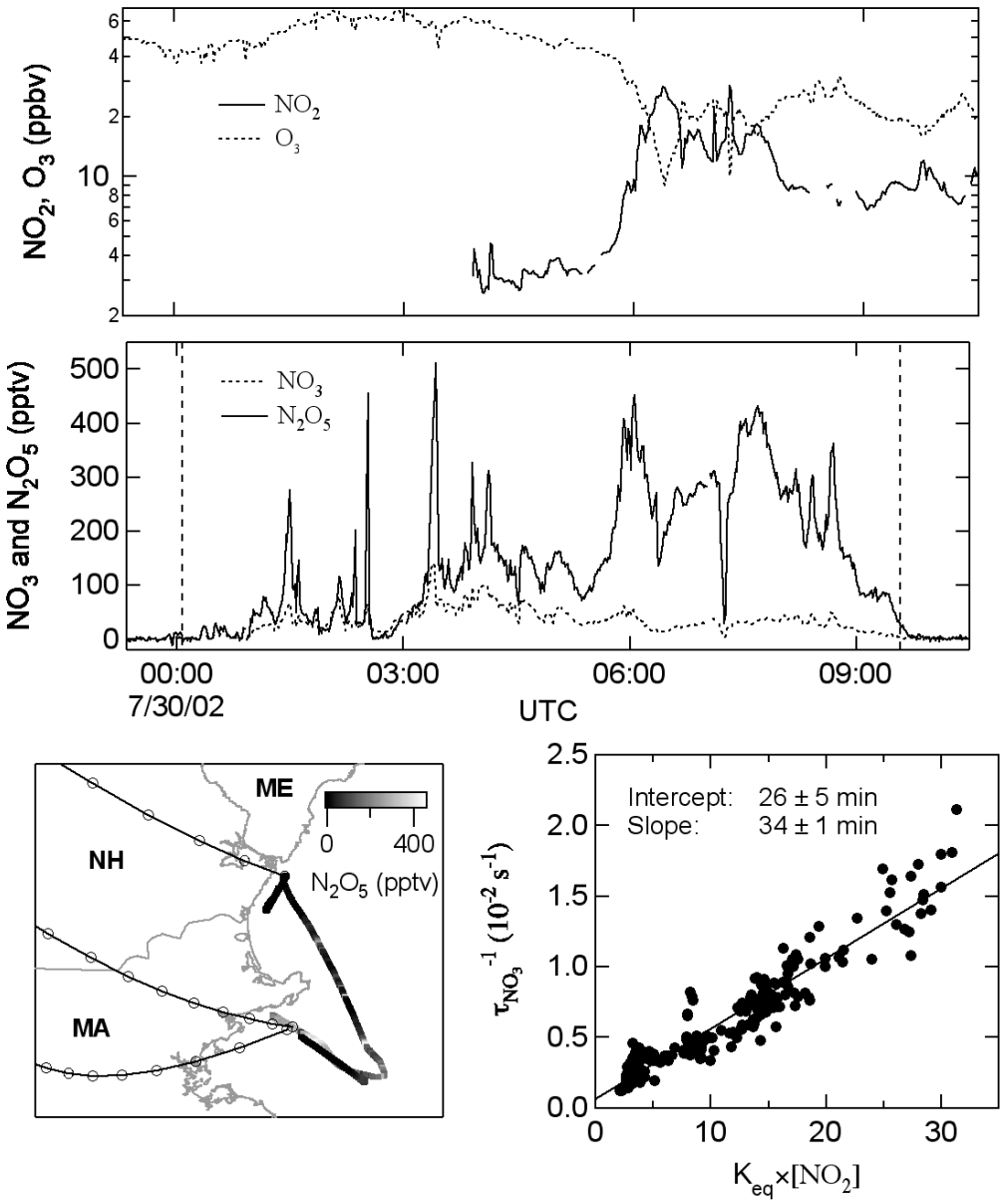

Figure 5 *Top*: Time series of NO_3, N_2O_5, NO_2 and O_3 mixing ratios. Time is in UTC, 4 hours offset from local time. Times of sunset and sunrise are marked. *Bottom Right:* Plot of $\tau_{NO_3}^{-1}$ vs. $K_{eq}[NO_2]$ as in equation (5) for the data from 3:55 – 9:30 UTC. The solid line is a linear fit ($r^2 = 0.82$) with the inverses of the slope and intercept shown in the legend. *Bottom Left;* Map showing the R/V *Brown* track on July 29-30, 2002, color coded according to the mixing ratio of N_2O_5. Lines with circles are the calculated back trajectories for the sampled air masses, with each point representing one hour upwind.

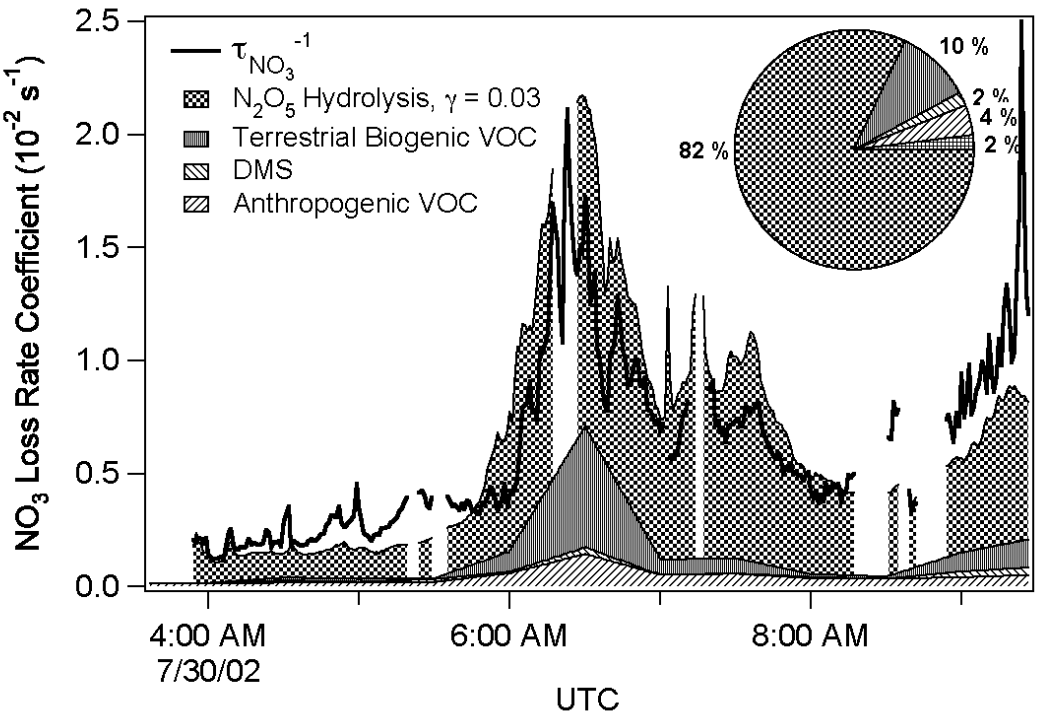

Figure 6 Comparison of observed and calculated values for the NO_3 first order loss rate coefficient for the data in Fig. 5. The calculated individual contributions from NO_3 reactions with anthropogenic VOC, terrestrially emitted biogenic VOC, and dimethyl sulfide from equation (7) and the measured VOC concentrations are stacked together as shown in the legend. Also included in the stacked sum is the NO_3 loss from N_2O_5 hydrolysis, i.e., $k_{N_2O_5} K_{eq}[NO_2]$, with $\gamma(N_2O_5) = 0.03$ in equation (8). The pie chart in the inset gives the average contributions of these loss rate coefficients to the averaged, total loss over the course of the night using the same code as the legend. The additional 2% slice on the pie chart includes heterogeneous NO_3 loss with $\gamma(NO_3) = 4\times10^{-3}$.

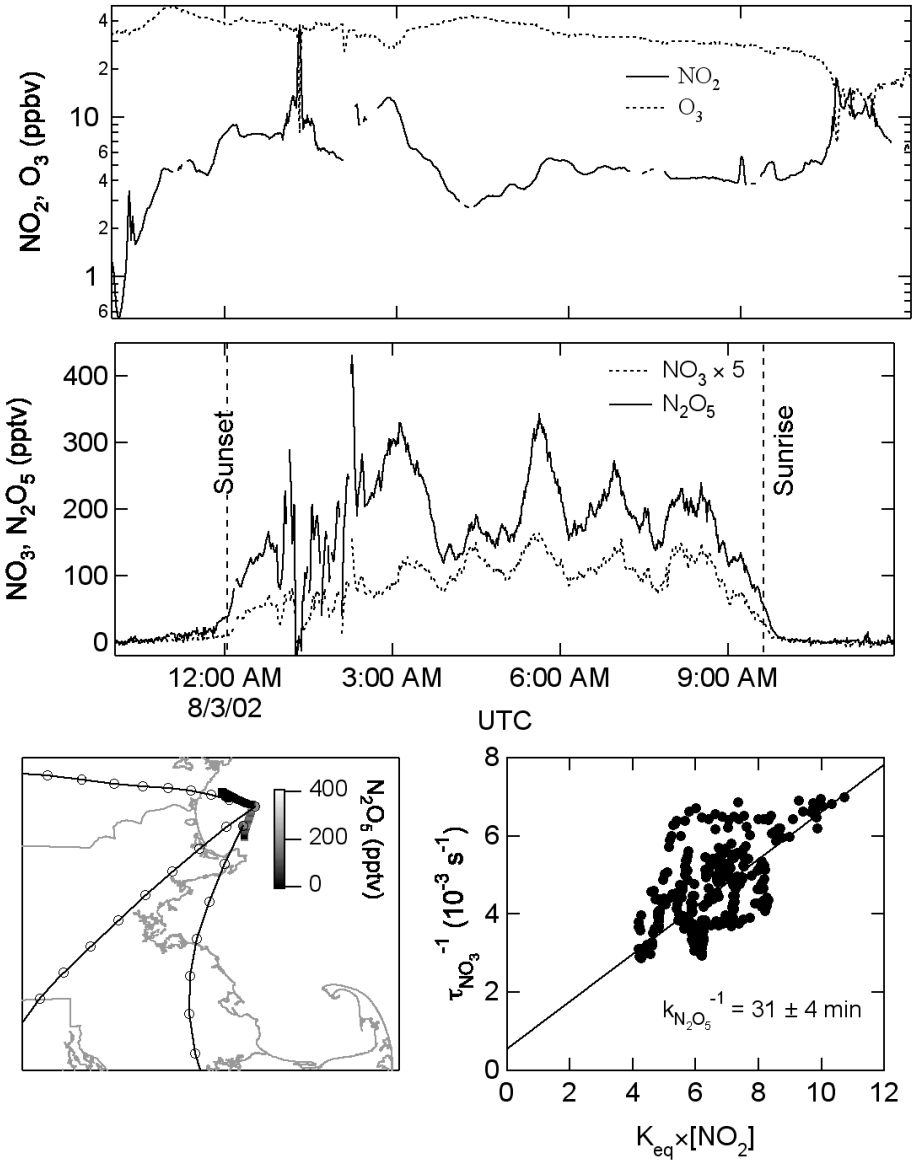

Figure 7. *Top:* Time series of NO_3, N_2O_5, NO_2 and O_3 for August 2-3, 2002, as in Fig. 5, except with the NO_3 mixing ratio multiplied by a factor of 5 to make it visible on the scale of the left axis. Times of sunrise and sunset are marked. *Bottom Right:* Plot of $\tau_{NO_3}^{-1}$ vs. $K_{eq}[NO_2]$. The solid lines is a linear fit, with the inverse of the slope and intercept shown on the graph. *Bottom Left:* Map showing the R/V *Brown* track in the Gulf of Maine, color coded according to the N_2O_5 mixing ratio. Lines with circles are back trajectories as in Figure 5.

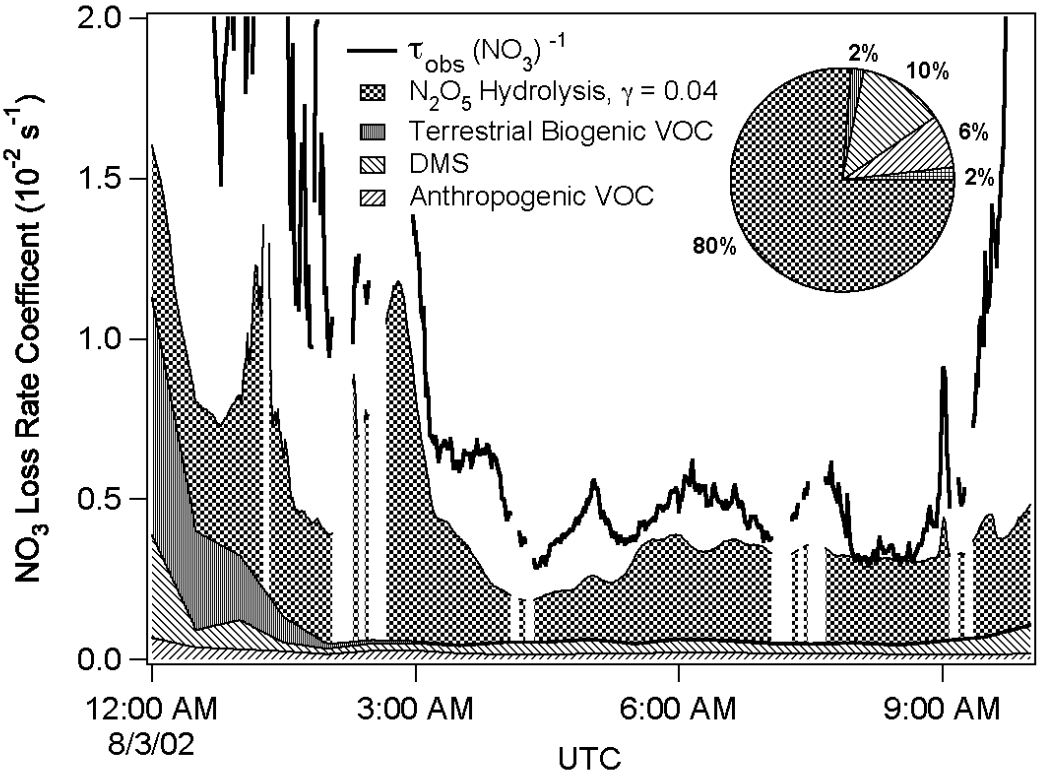

Figure 8. Comparison of observed and calculated NO_3 first order loss rate coefficient for the data in Fig. 7. The format of this figure is analogous to that of Fig. 6, except that $\gamma(N_2O_5) = 0.04$, as derived from Fig. 7. Note that the contribution of NO to the NO_3 and N_2O_5 loss, which is significant before 12:00, after 9:30 (i.e., during daylight) and for brief periods between 12:40-2:20, has been omitted. The pie chart in the inset shows the average of the calculated losses for the period between 2:20 and sunrise.

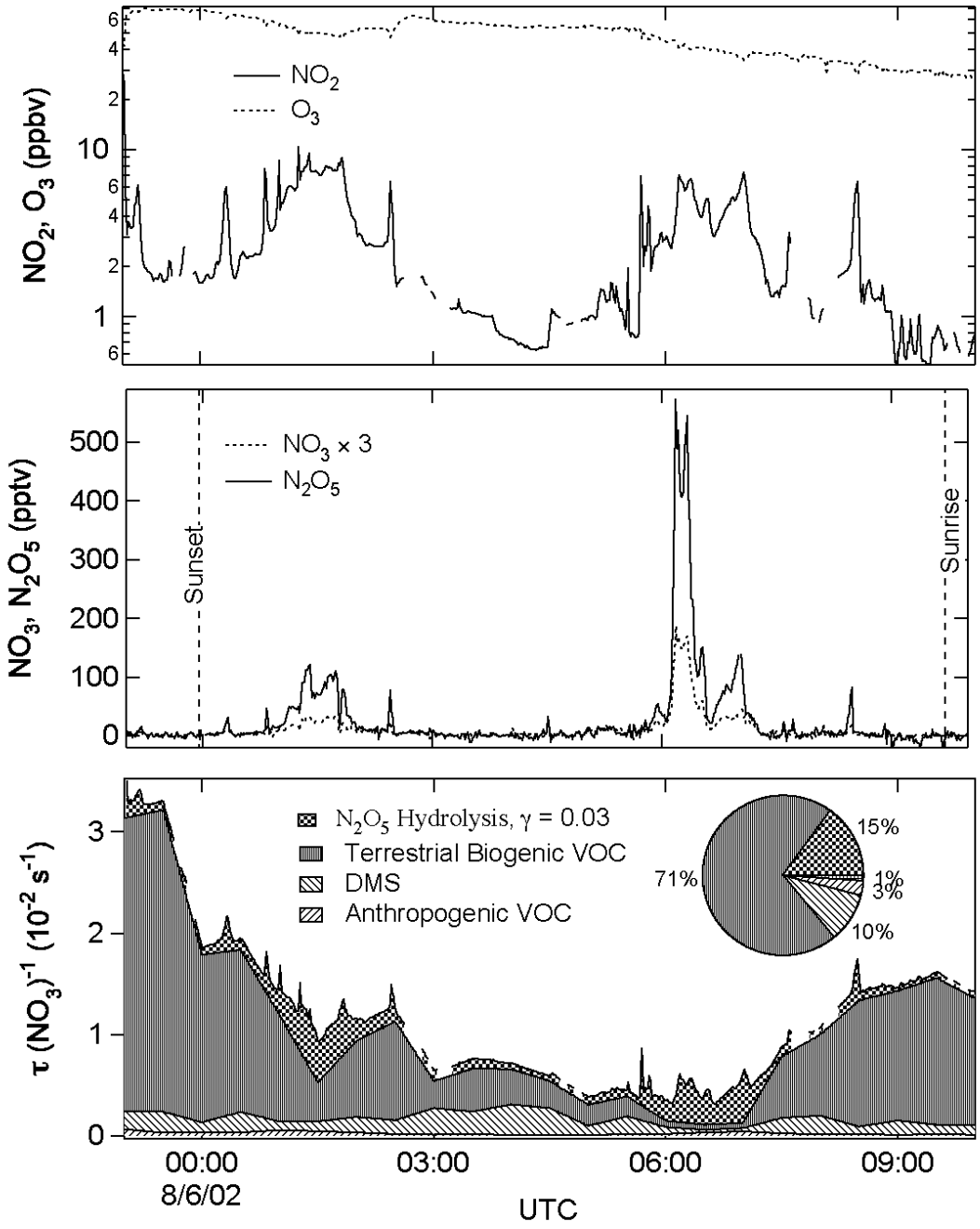

Figure 9. *Top:* Time series of NO_3, N_2O_5, NO_2 and O_3 for August 5-6, 2002, with NO_3 multiplied by a factor of 3. *Bottom:* Calculated NO_3 first order loss rate coefficient, $k_{NO_3}^{Calc}$, as in preceding figures The contribution of NO, present before sunset and after sunrise, is not shown. The pie chart on the inset shows the average contributions of each loss pathway for the period between sunset and sunrise.

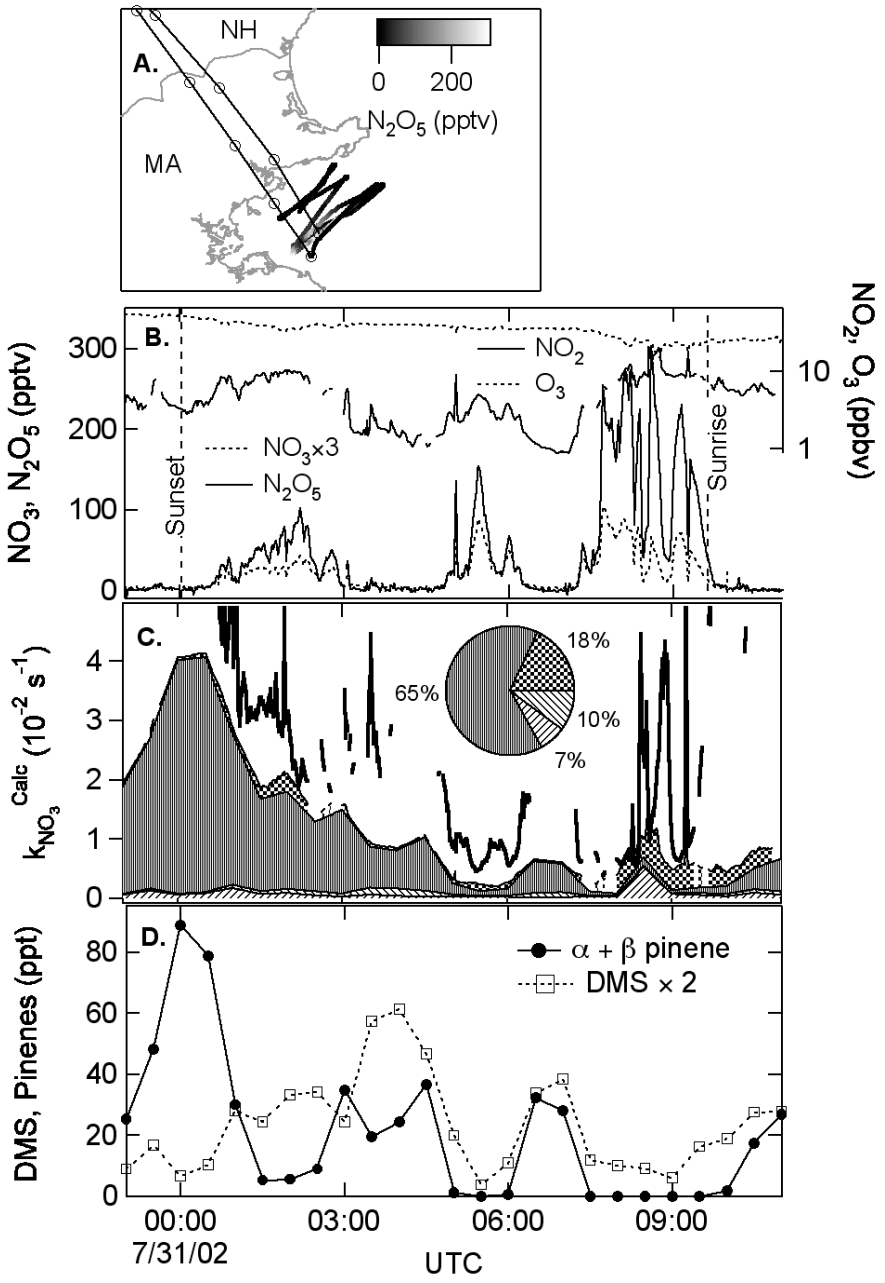

Figure 10. **A.** Map of R/V *Brown* track, shaded by the N_2O_5 mixing ratios, and calculated back trajectories. **B.** Time series from July 30-31 of NO_3, N_2O_5, NO_2 and O_3, with the NO_3 mixing ratio multiplied by a factor of 3. **C.** Calculated first order NO_3 loss rate coefficients, $k^{Calc}_{NO_3}$ showing the individual contributions. The pattern scheme is the same as in Figs. 6, 8 and 9, and the solid red line is $\tau_{NO_3}{}^{-1}$. The pie chart in the inset shows the average, relative contribution from each sink for the period between sunset and sunrise. **D.** Time series of α-pinene and DMS. The correlation between these compounds is driven their common sink via. NO_3 reaction.

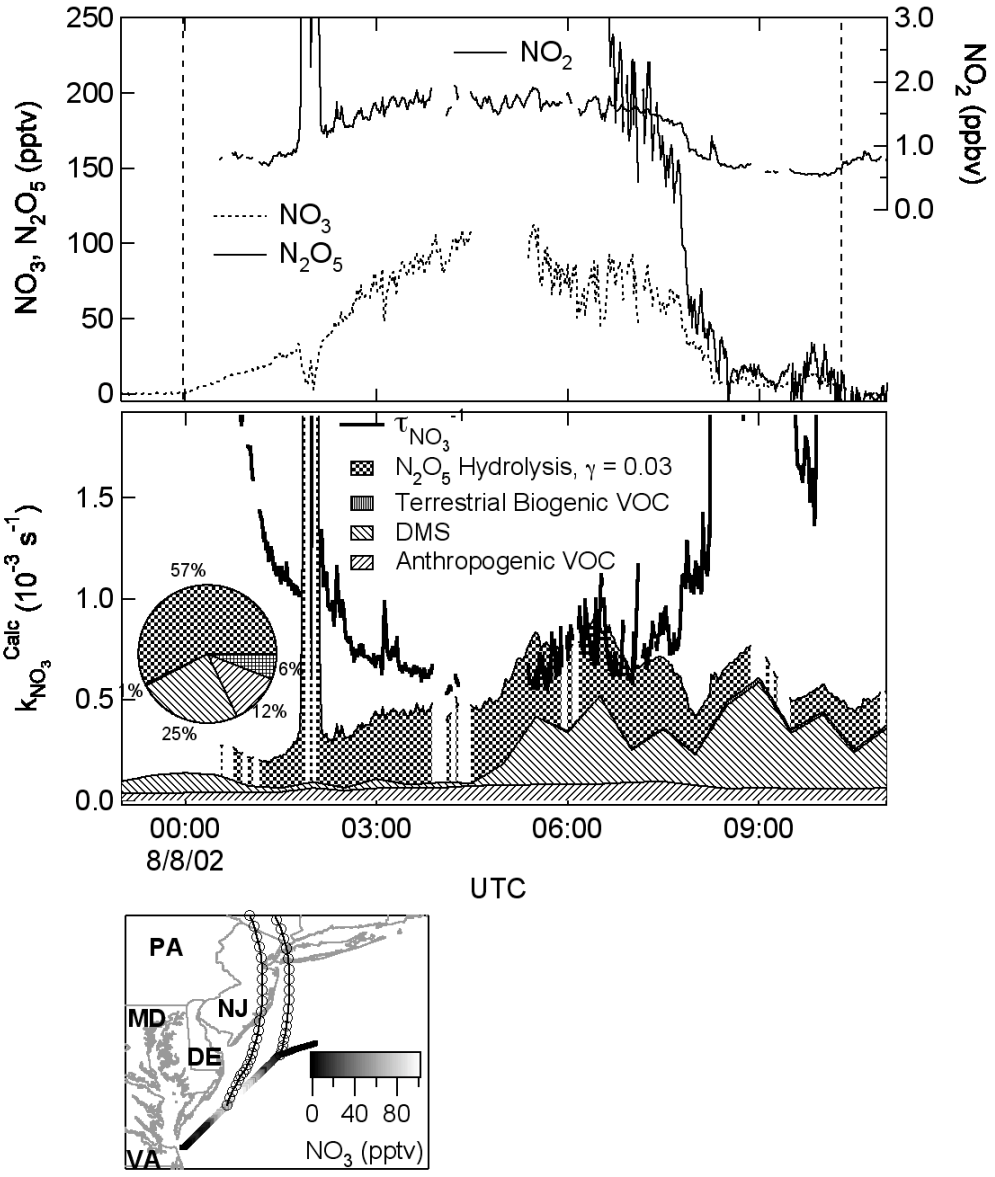

Figure 11. *Top:* Time series from August 7-8 of NO_3, N_2O_5 and NO_2. N_2O_5 was only available in the latter part of the night due to an instrumental difficulty. O_3 (not shown) was steady at 45 ppbv. *Middle:* Calculated first order NO_3 loss rate coefficients, $k_{NO_3}^{Calc}$ showing the individual contributions. The solid line is $\tau_{NO_3}^{-1}$. The pie chart at the bottom shows the averaged contributions to this loss between sunset and sunrise. *Bottom:* Map of the R/V *Brown* track shaded by the NO_3 mixing ratio. Back trajectories are shown, as in the preceding figures.

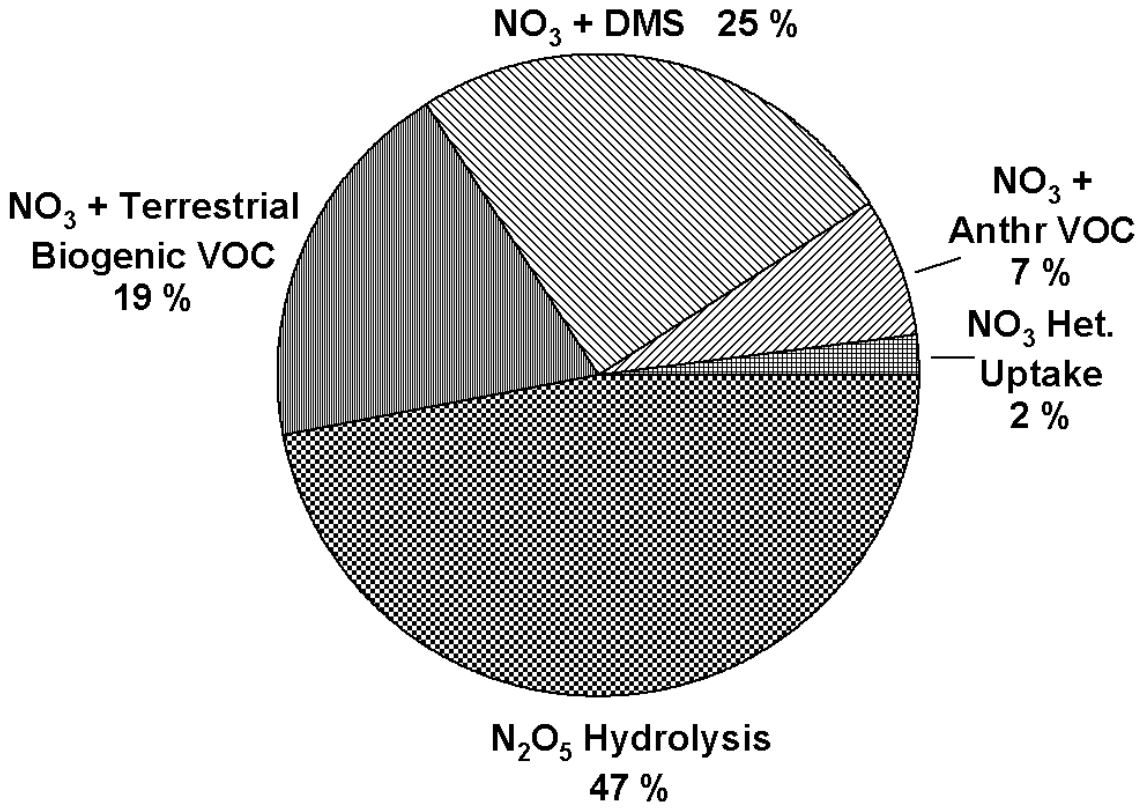

Figure 12. Fractional contributions to the reciprocal lifetime of NO_3 for the entire NEAQS 2002 campaign. Heterogeneous losses of NO_3 and N_2O_5 use constant values of 4×10^{-3} and 3×10^{-2} for the uptake coefficients, respectively. Variability in these uptake coefficients could change he partitioning of sinks considerably.

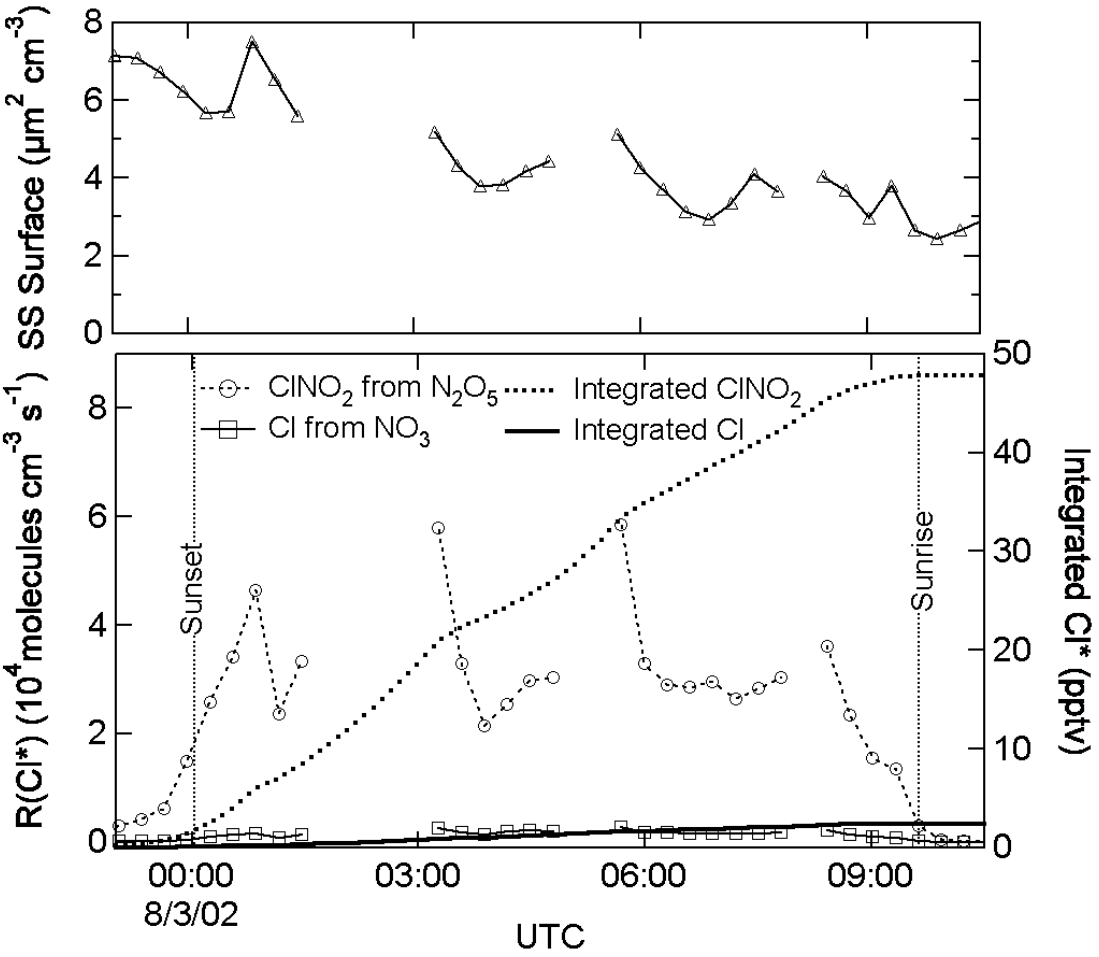

Figure 13. *Top:* Sea salt surface area calculated from the supermicron aerosol size distribution for August 2-3, 2002. *Bottom:* Calculated production rates for Cl containing compounds (R(Cl*), left axis) from NO_3 and N_2O_5 uptake on sea salt. The right axis shows the integrated Cl* yield in pptv assuming unit yield and zero loss.

Color Figures (2-13)

Figure 2.

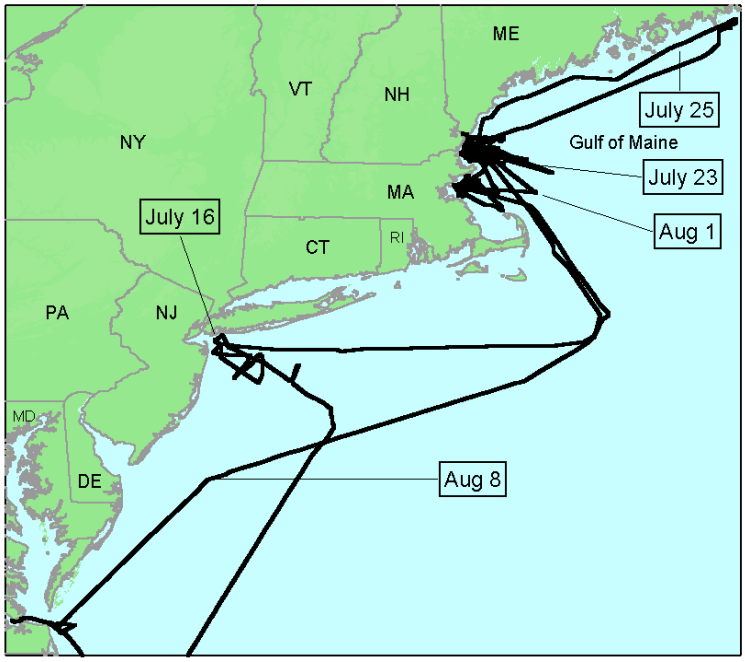

Figure 3.

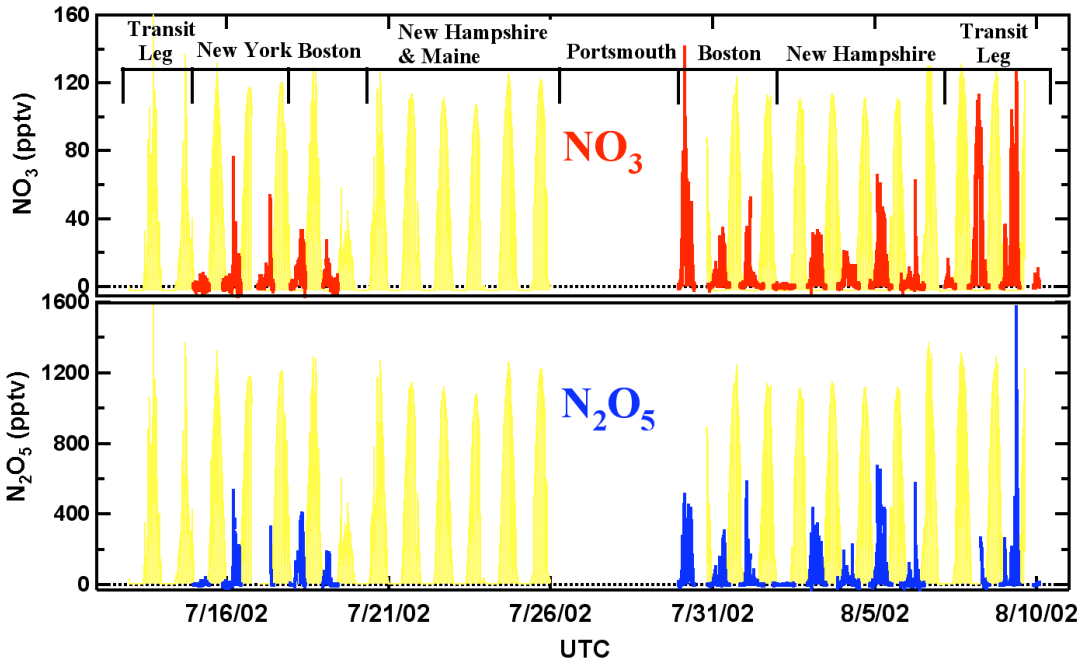

Figure 4.

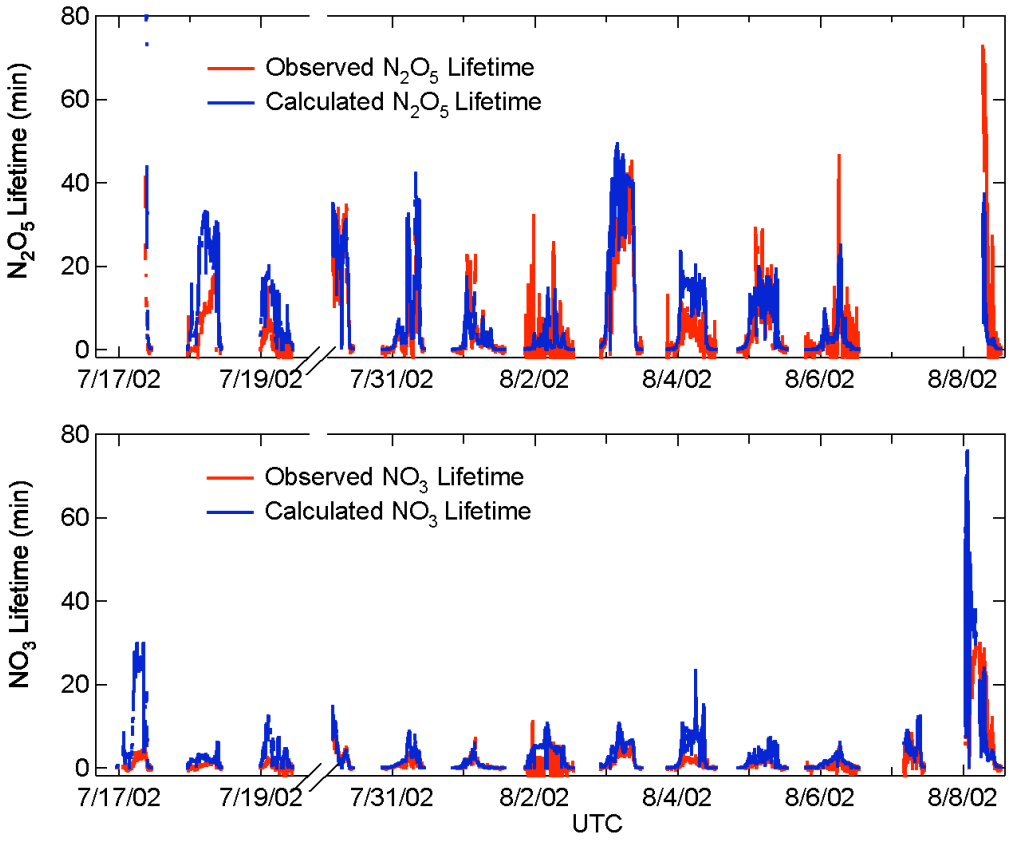
80
60
40
20
0
N_2O_5 Lifetime (min)
Observed N_2O_5 Lifetime
Calculated N_2O_5 Lifetime
7/17/02
7/19/02
7/31/02
8/2/02
8/4/02
8/6/02
8/8/02
80
60
40
20
0
NO_3 Lifetime (min)
Observed NO_3 Lifetime
Calculated NO_3 Lifetime
7/17/02
7/19/02
7/31/02
8/2/02
8/4/02
8/6/02
8/8/02
UTC

Figure 5.

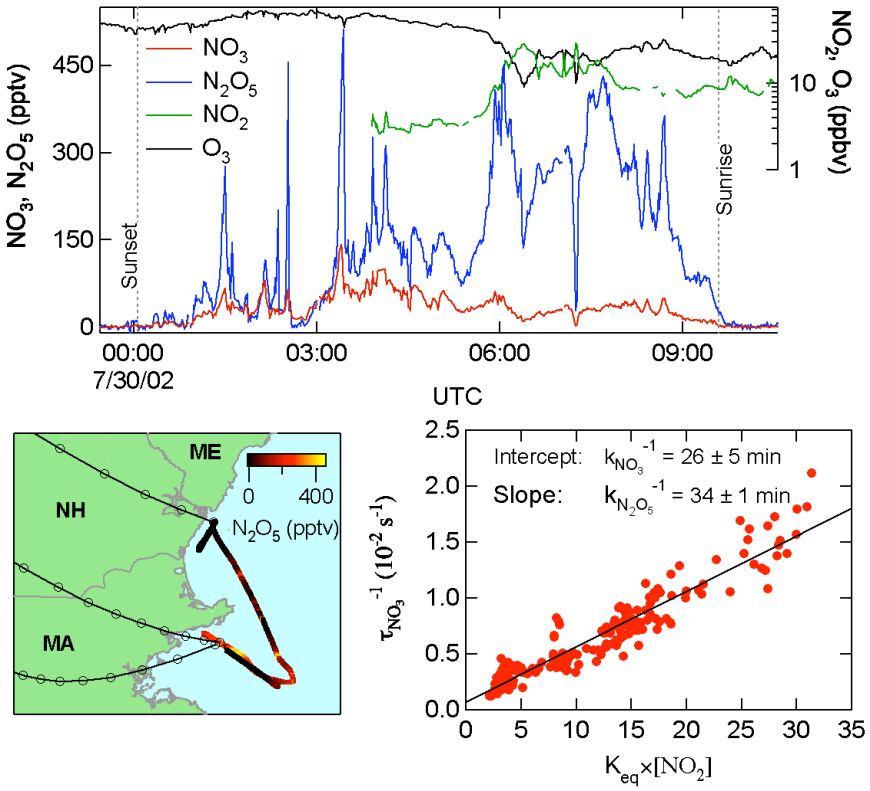

Figure 6.

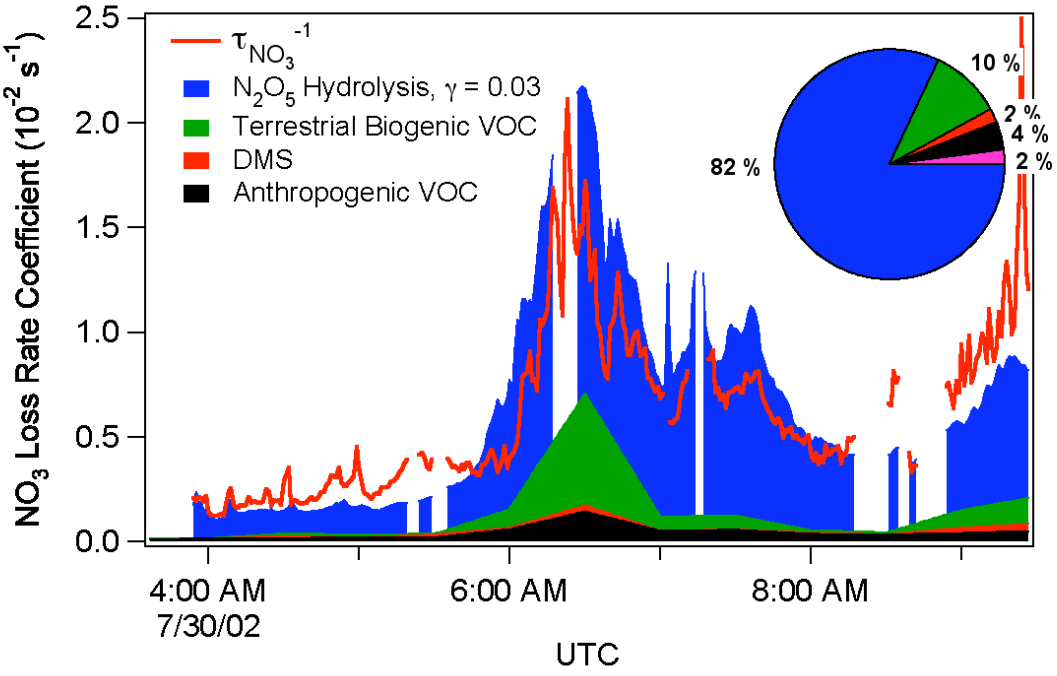

Figure 7.

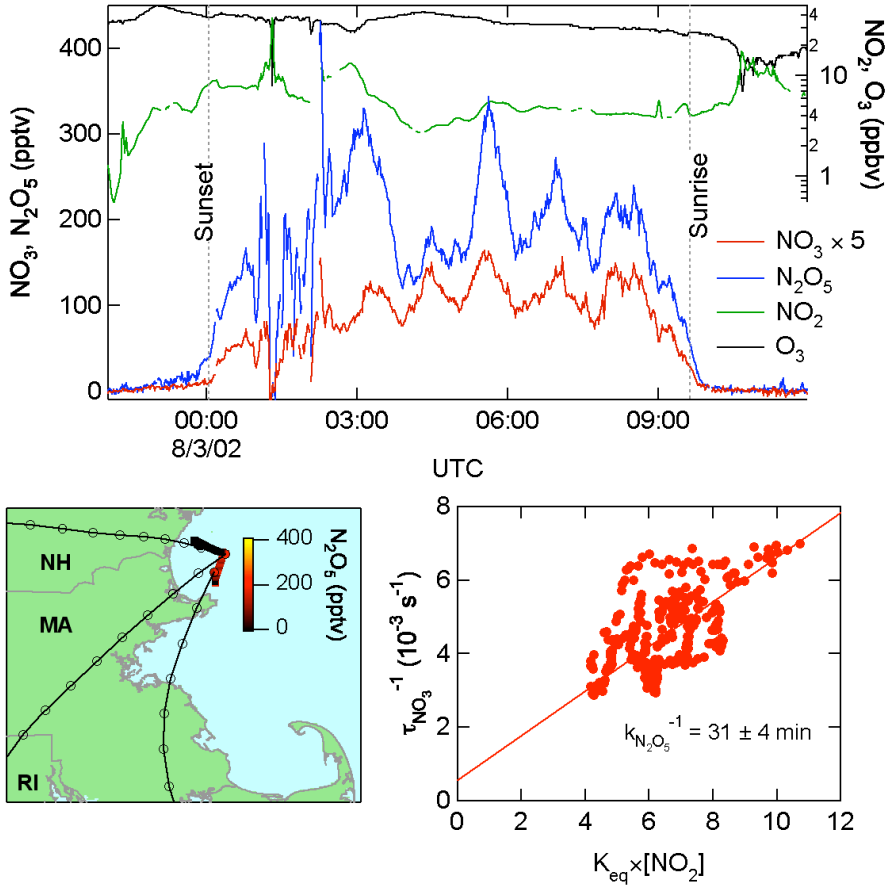

Figure 8.

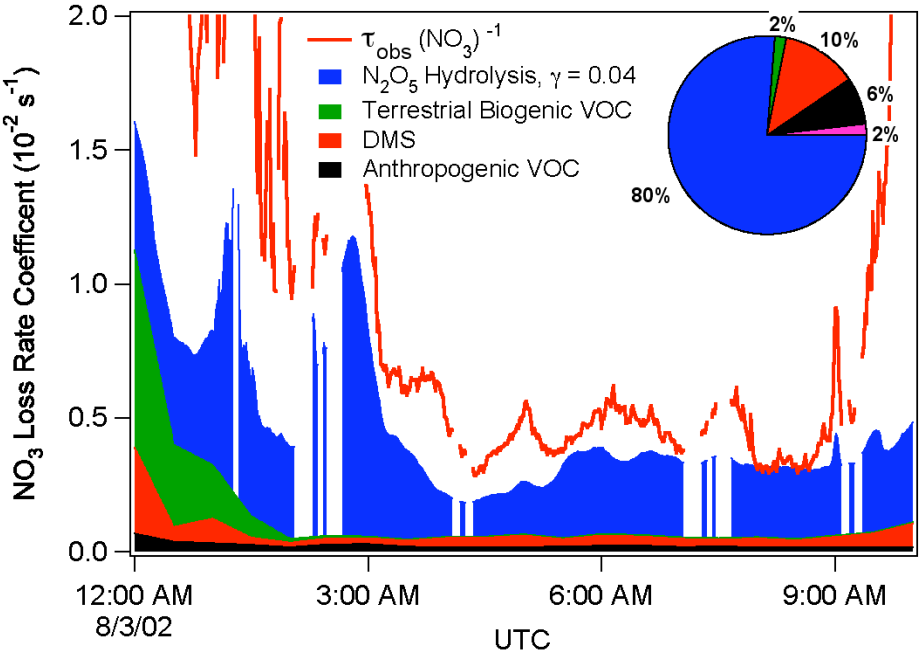

Figure 9.

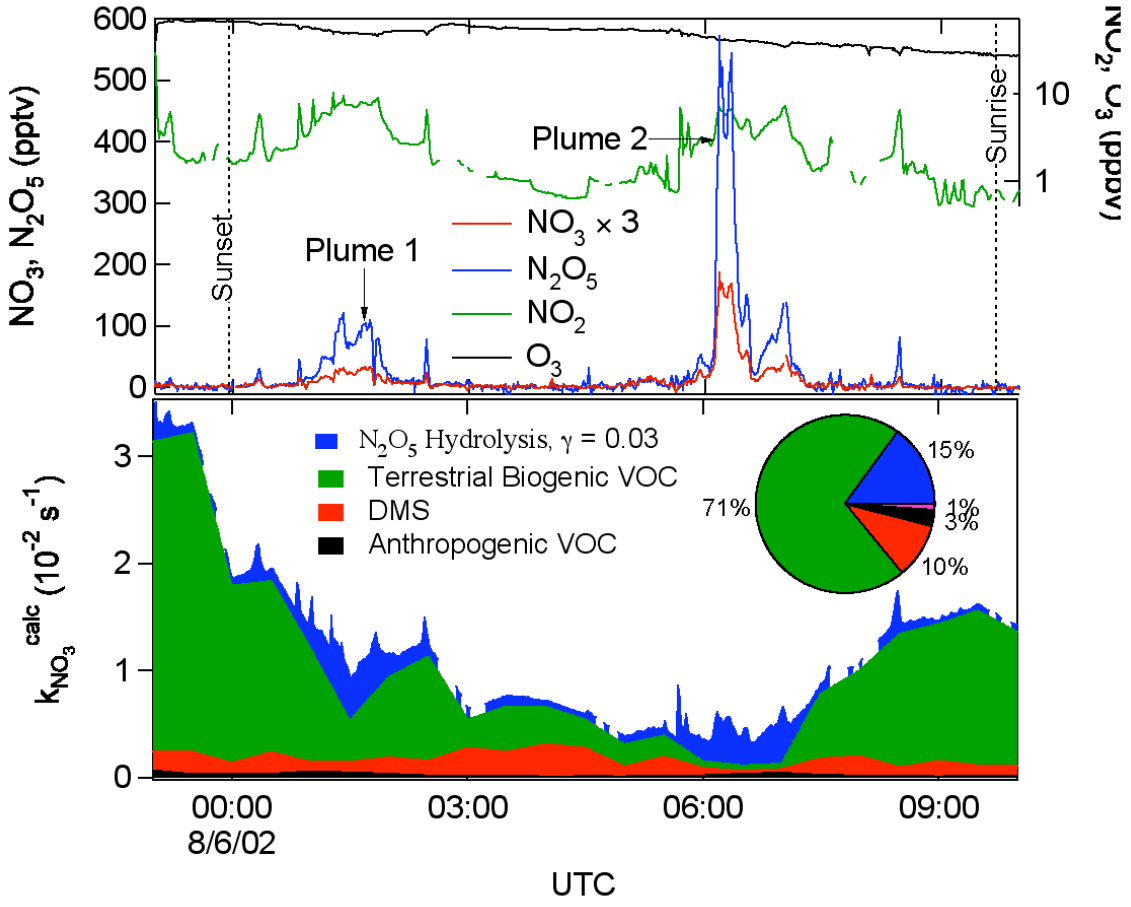
600
500
400
300
200
100
0
NO_3, N_2O_5 (pptv)
Sunset
Sunrise
Plume 1
Plume 2
NO_3 × 3
N_2O_5
NO_2
O_3
10
1
NO_2, O_3 (ppbv)
N_2O_5 Hydrolysis, γ = 0.03
Terrestrial Biogenic VOC
DMS
Anthropogenic VOC
15%
71%
1%
3%
10%
$k^{calc}_{NO_3}$ (10^{-2} s^{-1})
3
2
1
0
00:00
8/6/02
03:00
06:00
09:00
UTC

Figure 10.

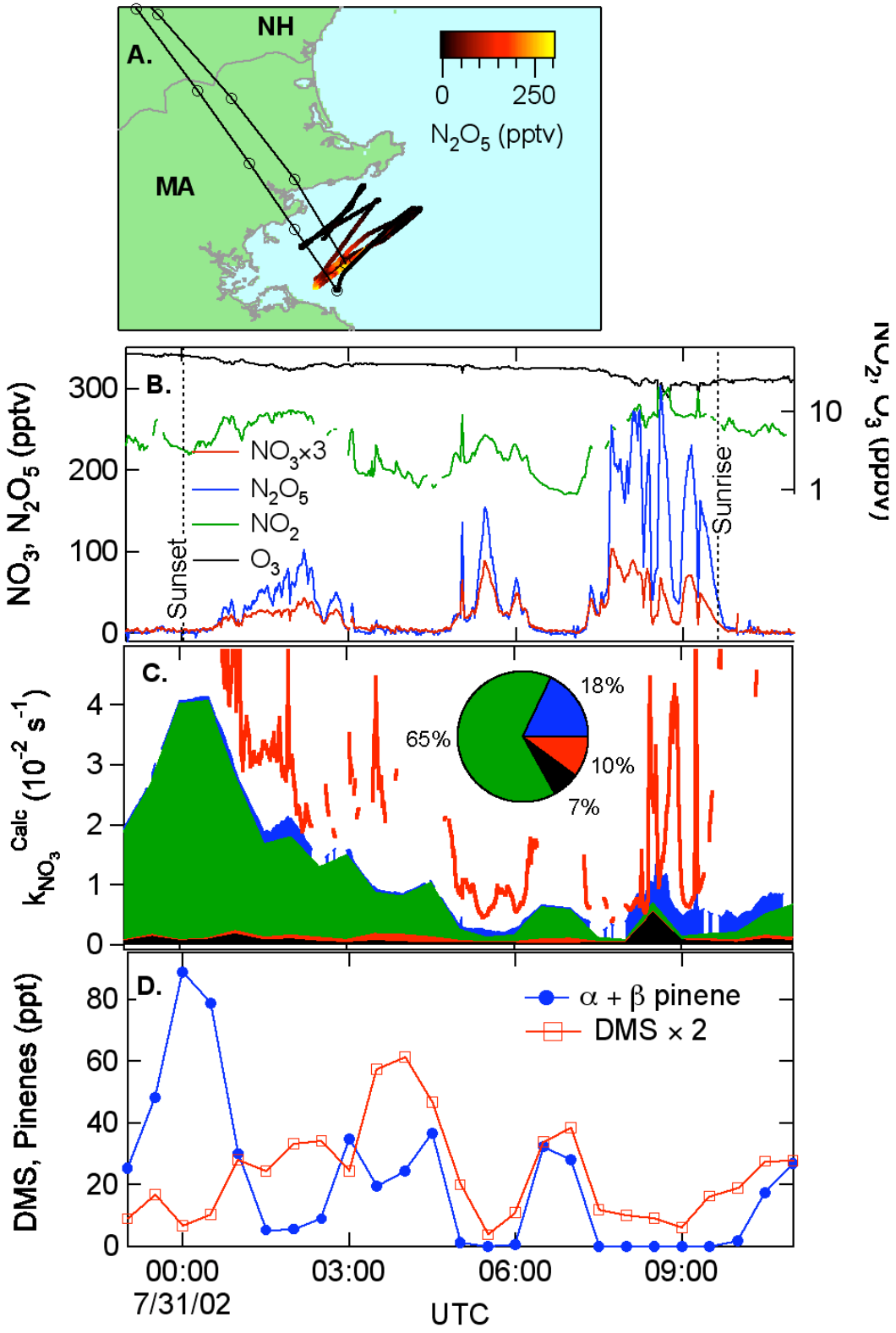
A.
NH
MA
0
250
N_2O_5 (pptv)
B.
NO_3, N_2O_5 (pptv)
300
200
100
0
NO_3x3
N_2O_5
NO_2
O_3
Sunset
Sunrise
10
1
NO_2, O_3 (ppbv)
C.
$k_{NO_3}^{Calc}$ (10^{-2} s^{-1})
4
3
2
1
0
18%
65%
10%
7%
D.
DMS, Pinenes (ppt)
80
60
40
20
0
α + β pinene
DMS × 2
00:00
7/31/02
03:00
06:00
09:00
UTC

Figure 11.

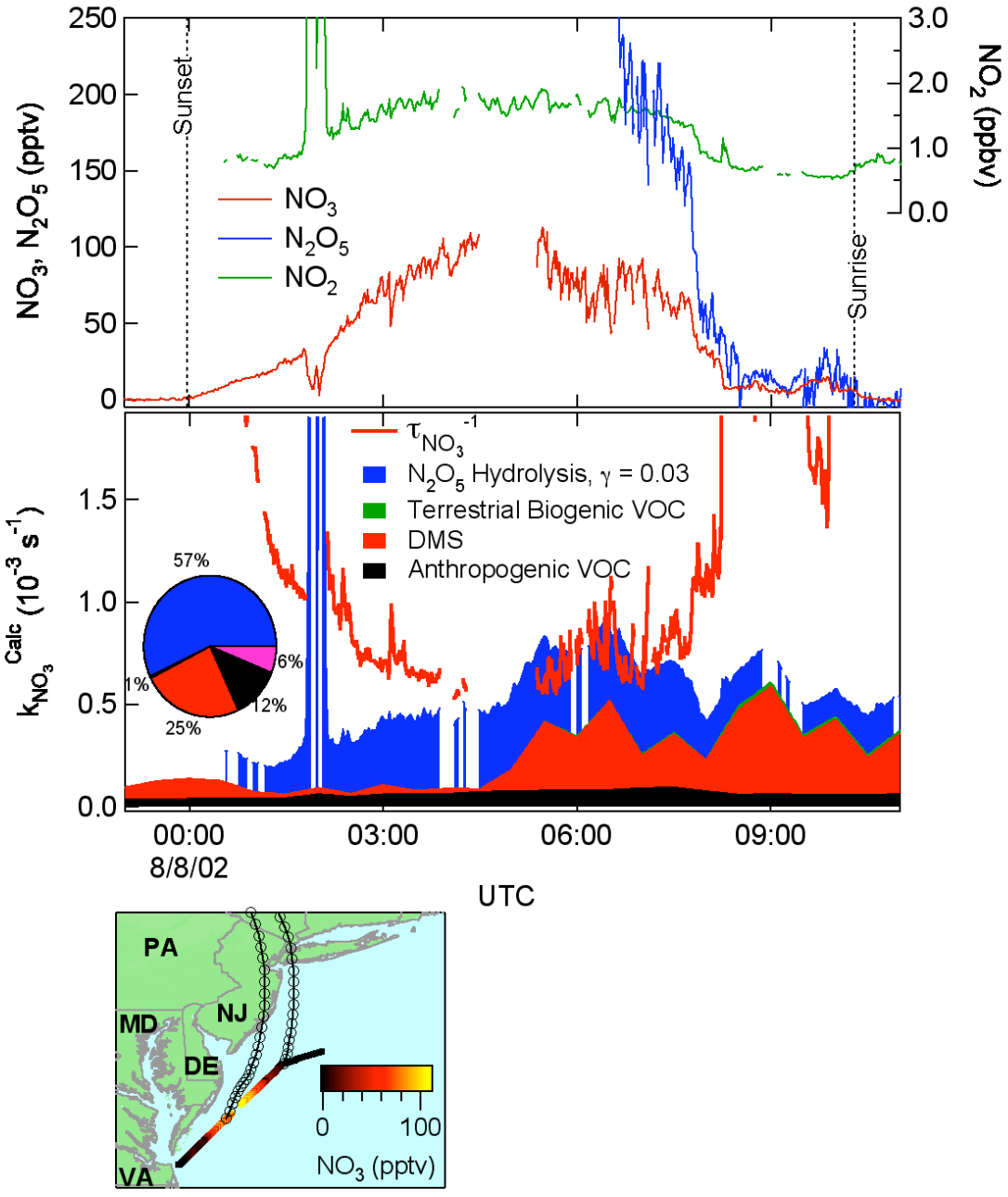
250
200
150
100
50
0
NO_3, N_2O_5 (pptv)
Sunset
Sunrise
NO_3
N_2O_5
NO_2
3.0
2.0
1.0
0.0
NO_2 (ppbv)
$\tau_{NO_3}^{-1}$
N_2O_5 Hydrolysis, γ = 0.03
Terrestrial Biogenic VOC
DMS
Anthropogenic VOC
57%
6%
1%
2%
25%
$k_{NO_3}^{Calc}$ (10^{-3} s^{-1})
1.5
1.0
0.5
0.0
00:00
8/8/02
03:00
06:00
09:00
UTC
PA
MD
NJ
DE
VA
0
100
NO_3 (pptv)

Figure 12.

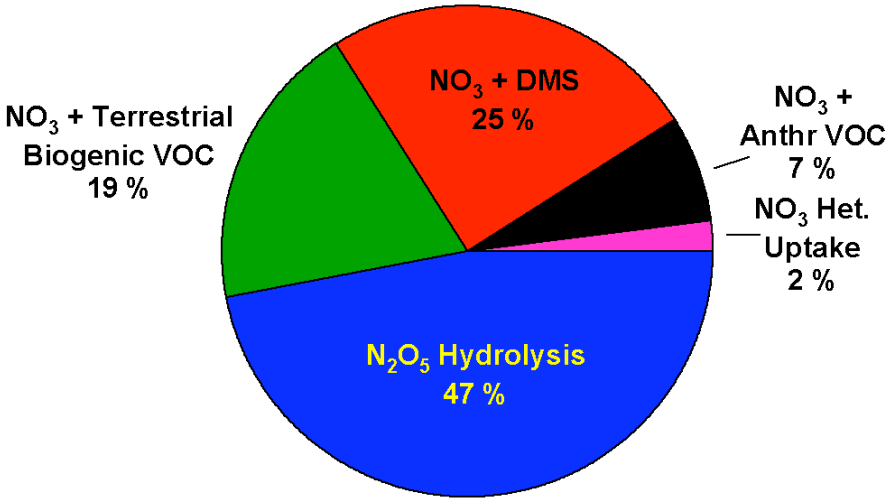

Figure 13.